Hyperfine Interactions 123/124 (1999) 367–399

Theoretical aspects of incoherent nuclear resonant scattering

W. Sturhahn [a] and V.G. Kohn [b]

[a] *Advanced Photon Source, Argonne National Laboratory, Argonne, IL 60439, USA*
[b] *Russian Research Centre "Kurchatov Institute", Moscow 123182, Russia*

The influence of nonrotational atomic motion on the scattering of X-rays by nuclei with sharp resonances is investigated. Two incoherent scattering channels, nuclear resonant fluorescence and nuclear resonant absorption followed by conversion electron emission and atomic fluorescence, are studied in detail. Time dependence and cross sections for these processes are given. In both cases, the cross section is proportional to the self-intermediate scattering function of the resonant isotope. The influence of other X-ray scattering processes on incoherent nuclear resonant scattering is discussed. We find that incoherent scattering channels dominate in off-resonance excitations. Self-intermediate scattering functions for the ideal gas and the harmonic lattice are calculated.

1. Introduction

The scattering and absorption of X-rays by an atom is usually dominated by contributions from the electrons. However, if the energy of the incident radiation is close to a nuclear resonance, the contribution of nuclear resonant scattering (NRS) becomes appreciable and may even dominate the electronic part. This became clear with the experiments of Mössbauer demonstrating recoilless nuclear absorption [1]. The discovery also prompted theoretical descriptions of coherent elastic NRS and related phenomena that arise from simultaneous scattering of all the nuclei or a particular subgroup of nuclei in a sample [2,3]. It was also suggested that NRS has the potential to probe phonon spectra [4–6], but the estimated cross-sections were too small to permit phonon spectroscopy with the existing radioactive sources. Amid the success of Mössbauer spectroscopy came the proposal by Ruby [7] to employ synchrotron radiation sources instead of a radioactive source. After the first experiments by Gerdau et al. [8], the novel approach was mainly used to explore coherent elastic scattering channels [9]. These experiments provided limited information about the lattice dynamics. The presence of atomic vibration merely reduces the elastic cross-section by the Lamb–Mössbauer factor, and the temperature variation of the second-order Doppler shift of the nuclear levels is observable. It is not possible to derive detailed information about the excitation spectrum of the lattice vibrations.

The knowledge of the dynamics of atomic motion has been very valuable in condensed matter physics [10]. Various techniques have been applied in this body of

research, with inelastic neutron scattering among the most popular. The application of NRS as a tool for investigations of lattice vibrations was pioneered by Seto et al. [11], Sturhahn et al. [12], and Chumakov et al. [13]. The novel method was readily applied to a variety of samples using different nuclear resonant isotopes [14–16]. This development became possible with the advent of highly brilliant synchrotron radiation sources more than 30 years after the idea was presented by theorists. Synchrotron radiation is observed as a series of very short flashes, and it is a characteristic feature of several nuclear resonances to respond with measurable time delay to such a flashlike excitation. This time structure permits the use of timing techniques to discriminate even extremely weak NRS from electronic scattering, and the basis for novel applications of NRS in condensed matter physics was established.

In comparison to coherent elastic NRS, the nature of incoherent NRS with synchrotron radiation has been investigated less comprehensively in the past. An early demonstration experiment by Cohen et al. [17] was followed by studies of incoherent emission of photons by Bergmann et al. [18] and by Baron et al. [19]. The interplay between coherent elastic and incoherent NRS observing conversion electrons was investigated by Sturhahn et al. [20]. Here we present a theoretical study of the time-dependent response of a thermalized ensemble of resonant nuclei to flashlike synchrotron radiation. We focus on nuclear resonant fluorescence and atomic fluorescence following conversion electron emission, which are incoherent scattering channels. This selection is motivated by the demonstrated potential for phonon spectroscopy.

In section 2, we outline some of the basic features of NRS and the relationship of nuclear resonances and atomic vibration. The different scattering channels are classified using quantum mechnical terminology. Section 3 concentrates on time dependence and strength of nuclear resonant fluorescence and atomic fluorescence following conversion electron emission for an individual atom. The lattice vibrations enter the description in terms of a self-intermediate scattering function [21], which is related to van Hove's self-correlation function [22] by Fourier transformation in space. The interplay between different X-ray scattering channels involving NRS is addressed in section 4. Even for macroscopic samples, NRS with energy transfer to atomic vibrations is dominated by the previously mentioned incoherent NRS channels. In section 5, we discuss the self-intermediate scattering function of the ideal gas and the harmonic lattice.

2. Basic aspects of NRS

NRS can be studied in the framework of quantum electrodynamics (QED) as a special case of the typical scattering situation [23]. The general Hamiltonian involves the free electromagnetic radiation, the free electromagnetic currents, and the electromagnetic interaction. Here we are mainly concerned with the interaction of X-ray photons with matter at ambient conditions. Photon field modes with typical X-ray energies do not strongly participate in the binding of atoms. This can be inferred from the high quality, i.e., the ratio of resonance energy to resonance width, of atomic resonances in the X-ray regime. Therefore it is justified to construct the bound atomic

states without high-energy modes of the photon field. The simplification for the treatment of the scattering process lies in the introduction of "dressed" charges, i.e., the charges are interacting via low-energy photons. This includes, e.g., the Coulomb interaction. The Hamiltonian is constructed accordingly by contributions from the dressed charges, $\widehat{H}_S$, the high-energy photon field modes, $\widehat{H}_R$, and the interaction between high-energy photon field modes and the dressed charges:

$$\widehat{H} = \widehat{H}_S + \widehat{H}_R + \widehat{H}_{\text{int}}. \tag{1}$$

Scattering problems are conveniently described in the interaction picture. In this representation, the time development of operators $\widehat{O}$ and state vectors $|\Psi\rangle$ is given by[1]

$$\frac{\mathrm{d}}{\mathrm{d}t}\widehat{O}(t) = \mathrm{i}\big[\widehat{H}_S + \widehat{H}_R, \widehat{O}(t)\big], \qquad \frac{\mathrm{d}}{\mathrm{d}t}\big|\Psi(t)\big\rangle = -\mathrm{i}\widehat{H}_{\text{int}}(t)\big|\Psi(t)\big\rangle. \tag{2}$$

As usual, the interaction Hamiltonian is expressed as[2]

$$\widehat{H}_{\text{int}}(t) = \int \hat{g}_\mu(\mathbf{x}, t)\hat{A}_\mu(\mathbf{x}, t)\,\mathrm{d}^3x \tag{3}$$

using the current operator $\hat{g}_\mu$ and the photon field operator $\hat{A}_\mu$. In our model, these operators describe the dressed charges and the high-energy field modes of the free photon field. In the covariant or Feynman gauge, the field operator $\hat{A}_\mu$ satisfies the homogeneous wave equation

$$\left(\nabla^2 - \frac{\partial^2}{\partial t^2}\right)\hat{A}_\mu = 0. \tag{4}$$

The simplicity of this equation is an advantage of working in the interaction picture. However, one has to realize that only the expectation values of the photon field operators can have physical meaning, and these expectation values will obey more complicated equations. In a scattering experiment, the conditions are typically chosen such that the interaction vanishes in the distant past and future, i.e., $\lim_{t\to\pm\infty}\widehat{H}_{\text{int}} = 0$. The initial and final states $|\Psi_{i,f}\rangle$ of the scattering process are then eigenstates of the non-interacting system and therefore time independent. They are related by a unitary transformation

$$|\Psi_f\rangle = \widehat{S}|\Psi_i\rangle, \quad \widehat{S} = T\exp\left\{-\mathrm{i}\int \widehat{H}_{\text{int}}(t)\,\mathrm{d}t\right\}, \tag{5}$$

where T symbolizes time ordering of operators. The modulo squared of the S-matrix elements $|\langle\Psi_f|\widehat{S}|\Psi_i\rangle|^2$ provides the probability of the scattering channel $|\Psi_i\rangle \to |\Psi_f\rangle$.

[1] Here and in the following expressions natural units, i.e., $\hbar = c = 1$, will be used.

[2] The four-vector conventions are adopted from [24], e.g., x is the four-vector $(t, \mathbf{x})$. Contractions of four-vectors are denoted as either $kx = k_0 t - \mathbf{k}\cdot\mathbf{x}$ or by repeated greek-letter indices $A_\mu B_\mu = A_0 B_0 - \mathbf{A}\cdot\mathbf{B}$.

For all practical purposes, X-ray photon fields encountered in NRS and other X-ray scattering are weak, and only one photon is involved. The scattering process is then sufficiently described by the one-photon propagator [25]

$$D_{\mu\nu}(x,y) = -\mathrm{i}\frac{\langle 0|T\widehat{S}\hat{A}_\mu(x)\hat{A}_\nu(y)|0\rangle}{\langle 0|\widehat{S}|0\rangle}. \tag{6}$$

In this expression, $|0\rangle$ denotes the "vacuum state" of the electromagnetic field, i.e., high-energy photons are absent. The operator $\widehat{S}$ is given in eq. (5). One can rewrite eq. (6) in terms of the one-photon propagator of the noninteracting photon field $D^0_{\mu\nu}$ and a matrix $M^{(fi)}_{\mu\nu}$ that describes the properties of the scatterer [23]:

$$D_{\mu\nu}(x,y) = D^0_{\mu\nu}(x-y) + \int D^0_{\mu\mu'}\big(x-x'\big)M^{(fi)}_{\mu'\nu'}\big(x',y'\big)D^0_{\nu'\nu}\big(y'-y\big)\,\mathrm{d}^4x'\,\mathrm{d}^4y'. \tag{7}$$

In the covariant or Feynman gauge, we write

$$D^0_{\mu\nu}(x) = \delta_{\mu\nu}\,\delta_+(x), \quad \delta_+(x) = -4\pi\lim_{\varepsilon\to+0}\int \frac{\mathrm{e}^{-\mathrm{i}kx}}{k^2+\mathrm{i}\varepsilon}\frac{\mathrm{d}^4k}{(2\pi)^4}. \tag{8}$$

The matrix elements $M^{(fi)}_{\mu\nu}$ are

$$M^{(fi)}_{\mu\nu}(x,y) = -\mathrm{i}\frac{\langle\Psi_f|T\widehat{S}\hat{j}_\mu(x)\hat{j}_\nu(y)|\Psi_i\rangle}{\langle\Psi_f|\widehat{S}|\Psi_i\rangle}, \tag{9}$$

where the initial and final system states $|\Psi_{i,f}\rangle$ do not contain X-ray photons. The occurrence of the operator $\widehat{S}$, which also contains photon field operators, is needed here to account for effects like the lifetime of excited states. The calculation of these matrix elements will of course depend on the particular scattering process under consideration. In the third section, we investigate incoherent scattering channels under the special conditions of NRS. Equation (7) exhibits a useful analogy to the vector potential of a classical electromagnetic field. If the one-photon propagator is convoluted with a transition current J_μ (a transition matrix element of a current operator), a classical vector potential is obtained. Imagine a localized transition current at a sufficient distance from the scatterer. The classical vector potential associated with the photon emitted by this transition current and incident on the scatterer is then transverse and described by

$$\mathbf{A}_0(x) = \frac{1}{4\pi}\int \delta_+(x-y)\mathbf{J}(y)\,\mathrm{d}^4y. \tag{10}$$

Clearly the transition current acts as the source of the field, which directly follows from the fact that δ_+ is a Green's function of the wave equation. The vector potential satisfies the inhomogeneous wave equation

$$\left(\nabla^2 - \frac{\partial^2}{\partial t^2}\right)\mathbf{A}_0(x) = -\mathbf{J}(x). \tag{11}$$

The same reasoning when applied to the convolution of eq. (7) with the transition current gives a transverse vector potential for the X-ray field at a sufficient distance from the scatterer:

$$\mathbf{A}_{fi}(x) = \int \delta_+(x-y)\,\mathbf{M}_{fi}\big(y,y'\big)\mathbf{A}_0(y')\,\mathrm{d}^4y\,\mathrm{d}^4y', \tag{12}$$

where the scattering matrix $\mathbf{M}_{fi}$ now relates only the transverse components of incident and scattered vector potentials. Equations (10) and (12) are the classical analogs of electromagnetic wave fields that contain just one photon. If the transition current in eq. (10) is localized in a small volume around $\mathbf{x} = 0$, the energy flux at a sufficiently distant point of observation $\mathbf{x}$ associated with each of these fields is obtained from the projection of the Poynting vector onto the direction of $\mathbf{x}$:

$$-\frac{1}{4\pi}\frac{\mathbf{x}}{|\mathbf{x}|}\cdot\Re\left(\frac{\partial\mathbf{A}}{\partial t}\times\nabla\times\mathbf{A}^*\right). \tag{13}$$

For a quasimonochromatic wave of average energy ω_0, one approximates $\partial\mathbf{A}/\partial t = -\mathrm{i}\,\omega_0\mathbf{A}$, and for large distances $|\mathbf{x}|$ the approximation $\mathbf{x}\cdot(\mathbf{A}\times\nabla\times\mathbf{A}^*) = -\mathrm{i}\omega_0|\mathbf{x}|\,|\mathbf{A}|^2$ can be used. From eq. (13) and these approximations, we obtain for the probability per unit time that the photon may be observed in the solid angle $\mathrm{d}\Omega$ and direction $\mathbf{x}/|\mathbf{x}|$:

$$\frac{\mathrm{d}^2P_{fi}}{\mathrm{d}\Omega\,\mathrm{d}t} = \frac{\omega_0}{4\pi}|\mathbf{x}|^2|\mathbf{A}_{fi}|^2. \tag{14}$$

We obtained this expression proceeding on the assumptions that the vector potential is a quasimonochromatic wave observed at a distance $|\mathbf{x}|$ much larger than the typical wavelength and much larger than the typical spatial extension of the source of the field. The indices $i,\ f$ refer to initial and final states of the scattering system. There is also a dependence on the properties of the incident radiation. Averaging over such properties will become necessary to accommodate practical situations.

The calculation of the scattering matrix from eq. (9) must consider all electromagnetic charges and currents of the scatterer, but we may introduce some reasonable assumptions to achieve a simplification of the problem. Most of the charges are organized in larger units, nuclei with core electrons, which are well localized. In addition, we find a small number of itinerant electrons. Accordingly we write the current operator $\hat{g}_\mu$ as a sum of the localized electronic currents $\hat{s}_\mu$, the intrinsic currents of the nuclei, $\hat{j}_\mu$, and a contribution from the itinerant electrons:

$$\hat{g}_\mu(\mathbf{x}) = \hat{s}'_\mu(\mathbf{x}) + \sum_p \big(\hat{s}^{(p)}_\mu\big(\mathbf{u}_p+\hat{\mathbf{r}}_p\big) + \hat{j}^{(p)}_\mu\big(\mathbf{u}_p+\hat{\mathbf{r}}_p\big)\big). \tag{15}$$

The operators $\hat{\mathbf{r}}_p$ describe the motion of the center of mass of each atom, and we assume these motions to be nonrelativistic. The vectors $\mathbf{u}_p$ assume the meaning of relative coordinates. The sum runs over all atoms in the scatterer. The initial and final states of the scattering process are eigenstates of the noninteracting system, and

it will be useful to discuss the eigenstates of the scattering system in more detail. The Hamiltonian of the scatterer may be approximated by the expression

$$\widehat{H}_S = \sum_p \widehat{H}_N^{(p)} + \widehat{H}_L + \widehat{H}_E + \widehat{V}, \tag{16}$$

where the $\widehat{H}_N$ give the intrinsic properties of ion cores, $\widehat{H}_L$ contains kinetic and potential energies of the center of mass of the ion cores, and $\widehat{H}_E$ describes degrees of freedom of the itinerant electrons. The contribution $\widehat{V}$ represents interactions between vibrations of the ion cores and the electrons. Time-dependent hyperfine interactions, i.e., an interaction term between intrinsic nuclear variables and electrons, were neglected. The system's eigenstates are then constructed from intrinsic eigenstates of the ion cores $|\phi\rangle$, eigenstates of the vibrating ion cores coupled to the electrons, $|\chi\rangle$, and eigenstates of the photon field:

$$|\mathbf{\Psi}\rangle = |\gamma\rangle|\chi\rangle \prod_p \left|\phi^{(p)}\right\rangle. \tag{17}$$

The probabilities for a scattering channel $|\mathbf{\Psi}_i\rangle \rightarrow |\mathbf{\Psi}_f\rangle$ are obtained from the S-matrix elements in eq. (5). The solution of the original problem stated in eq. (2) is equivalent to the expansion of the S-matrix elements in powers of the interaction Hamiltonian. The lowest order relevant to NRS is quadratic [23]. For the classification of the dominant scattering channels, we investigate the current–current matrix element

$$\begin{aligned}\left(\hat{g}_\mu \hat{g}_\nu\right)_{fi} = \langle\chi_f| \prod_l \left\langle\phi_f^{(l)}\right| \left(\hat{s}'_\mu + \sum_p \left(\hat{s}_\mu^{(p)} + \hat{j}_\mu^{(p)}\right)\right) \\ \times \left(\hat{s}'_\nu + \sum_p \left(\hat{s}_\nu^{(p)} + \hat{j}_\nu^{(p)}\right)\right) |\chi_i\rangle \prod_l \left|\phi_i^{(l)}\right\rangle.\end{aligned} \tag{18}$$

The contributions with only electronic currents are not relevant at this point. The terms containing nuclear and electronic currents were interpreted as "screening effects" and shown to be negligible in most cases [23,26]. Finally, in the purely nuclear contribution, "mirror terms" that contain current operators of two different nuclei can be neglected [23], and the dominant contribution to NRS remains

$$\begin{aligned}&\prod_{ll'} \langle\chi_f| \left\langle\phi_f^{(l)}\right| \sum_p \hat{j}_\mu^{(p)} \hat{j}_\nu^{(p)} \left|\phi_i^{(l')}\right\rangle |\chi_i\rangle \\ &\quad = \sum_p \langle\chi_f| \left\langle\phi_f^{(p)}\right| \hat{j}_\mu^{(p)} \hat{j}_\nu^{(p)} \left|\phi_i^{(p)}\right\rangle |\chi_i\rangle \prod_{l\neq p} \left\langle\phi_f^{(l)}\middle|\phi_i^{(l)}\right\rangle.\end{aligned} \tag{19}$$

With the help of this matrix element, NRS processes can be classified. Figure 1 contains the classification scheme to which we will adhere. In coherent scattering processes, the final states of all ion cores are identical to their initial states. Initial and final states of the vibrations and delocalized electrons define whether the process is elastic or inelastic. In either case, the scattering amplitudes from the individual ion cores

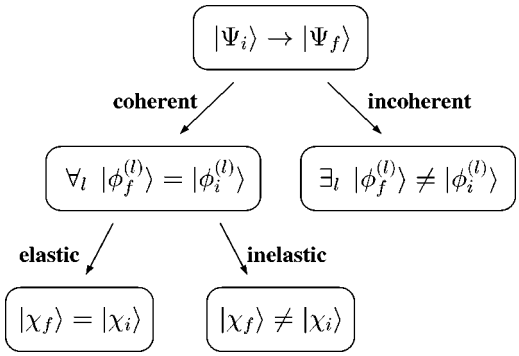

Figure 1. Classification scheme for NRS processes. The classification is based on initial and final quantum states of the scatterer. Incoherent scattering implies energy transfer to the photon field unless degenerate core states exist.

have to be added. The scattering process is called incoherent if at least one core state changes. Incoherent scattering therefore implies energy transfer unless degenerate core states exist, e.g., nonsplit nuclear ground states. In this case, the scattered intensities from the individual ion cores have to be added. The matrix elements follow from eq. (19):

$$\begin{aligned} \text{coherent:} \quad & \textstyle\sum_p \langle\chi_f|\langle\phi_i^{(p)}|\hat{j}_\mu^{(p)}\hat{j}_\nu^{(p)}|\phi_i^{(p)}\rangle|\chi_i\rangle, \\ \text{incoherent:} \quad & \langle\chi_f|\langle\phi_f^{(p)}|\hat{j}_\mu^{(p)}\hat{j}_\nu^{(p)}|\phi_i^{(p)}\rangle|\chi_i\rangle. \end{aligned} \tag{20}$$

In the first line, the sum over all atoms may lead to a coherent enhancement under particular scattering conditions. We note that the same classification is applicable to X-ray scattering by core electrons. Although we explained the classification scheme using the second-order S-matrix element, the arguments are easily extendible for higher order terms.

3. Incoherent NRS

In the previous section, incoherent NRS processes were defined in basic terms. There are many possible incoherent scattering channels that can be observed experimentally. The following scenarios were investigated:

(a) *Nuclear resonant fluorescence*.
The incident photon is absorbed and reemitted by the nuclear current. The resonant contribution of this process is displayed in figure 2(a). The vertices are constructed with nuclear currents according to eq. (15), i.e., lattice vibrations are included. The initial and final states of the nucleus must be different to produce incoherent scattering. This scattering channel was utilized to obtain the phonon density of states [27,28]. In macroscopic scatterers, multiple scattering channels involving coherent elastic processes may complicate the situation [19,29].

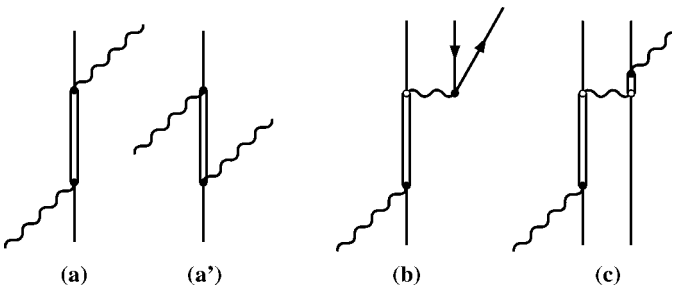

Figure 2. Incoherent NRS processes for the study of lattice vibrations. Nuclear resonant fluorescence (a), nonresonant nuclear fluorescence (a'), conversion electron emission (b), and atomic fluorescence following nuclear absorption (c) are depicted. The wavy lines symbolize X-ray photons, and the solid lines represent nuclear states. In panel (c), the right-hand side solid line stands for the electronic state of an atom, and the emission of the conversion electron is not explicitly shown. The contribution from diagram (a') is negligible. Only the vertices that connect to incoming and outgoing particles have to be calculated with the inclusion of atomic vibrations.

(b) *Conversion electron emission.*
After absorption of the incident photon by the nuclear current, a virtual photon transfers the excitation energy to the electron shell. An electron is emitted, and the hole remains bound in the ion core. The situation is illustrated in figure 2(b). Two of the three vertices are constructed including atomic motion. If the energy of the incident photon is close to the nuclear resonance, the interplay with coherent elastic NRS becomes important [20,30]. Investigations of lattice vibrations were also performed [31].

(c) *Atomic fluorescence following nuclear absorption.*
After a conversion electron has been emitted, the remaining ion core will de-excite rapidly. A large fraction of these de-excitations result in emission of fluorescence radiation. The scattering diagram is shown in figure 2(c). This scattering channel was used in various experiments aimed at the study of lattice vibrations [14–16].

All of the processes listed above are suitable for probing lattice vibrations. In this paper, we focus on processes (a) and (c) motivated by their feasibility in experiments. The calculation of the emitted photon fields from a single atom permits the derivation of time- and angle-dependent intensities. Effects due to multiple scattering in a macroscopic scatterer containing many atoms will be discussed later.

3.1. Nuclear resonant fluorescence

The evaluation of the scattering matrix defined by eq. (9) has been discussed extensively in the past. The perturbation expansion of the operator $\widehat{S}$ defined by eq. (5) in combination with time ordering produces a multitude of individual terms. From a physical standpoint this is plausible because the eigenstates of the charge distribution are not simply given by the eigenstates of the noninteracting system. They rather develop slowly from the distant past when the interaction is "switched on" according

to eq. (2). One starts with the general expression given by eq. (9) and assumes that the spectrum of the incident field in eq. (12) is close to a narrow nuclear resonance. Those terms of the scattering matrix that contribute to the scattered field are then well described by the "ladder approximation". A derivation of the scattered vector potential for this case has been given earlier by Hannon and Trammell [23]. The scattering matrix takes the form

$$\mathbf{M}_{fi}(x,x') = -\mathrm{i}\lim_{t_0\to\infty}\langle\chi_f|\langle\phi_f|\widehat{G}'(t_0-t)\hat{\mathbf{j}}(\mathbf{x})\widehat{G}'(t-t')\hat{\mathbf{j}}(\mathbf{x}')\widehat{G}'(t'-t_0)|\phi_i\rangle|\chi_i\rangle, \quad (21)$$

where the operator $\widehat{G}'$ only propagates into the future, i.e., $\widehat{G}'(t-t')=0$ for $t<t'$. The construction of $\widehat{G}'$ involves virtual photon exchange between currents within the atom, and the period of time that elapses between emission and absorption of a virtual photon is determined by the size of the atom. Therefore, one can neglect atomic vibrations during virtual photon exchange. It is then possible to write $\widehat{G}'(t)=\widehat{U}_L(t)\widehat{G}(t)=\widehat{G}(t)\widehat{U}_L(t)$, where the time development operator of the lattice, $\widehat{U}_L(t)=\exp(-\mathrm{i}(\widehat{H}_L+\widehat{H}_E+\widehat{V})t)$, is obtained from eqs. (2) and (16). $\widehat{G}$ is discussed in detail in appendix A and does not operate on the lattice states $|\chi\rangle$. Nuclear intrinsic properties and the effect of atomic vibrations are now conveniently separated by introducing the space Fourier transform[3] $\widehat{\mathbf{J}}(\mathbf{k})$ of the transverse current operator $\hat{\mathbf{j}}(\mathbf{x})$ in the center of mass system, i.e., $\widehat{\mathbf{J}}$ does not operate on the lattice states. We use the operator $\hat{\mathbf{r}}$ to describe the motion of the center of mass of the atom and write

$$\hat{\mathbf{j}}(\mathbf{x}) = \int \mathrm{e}^{-\mathrm{i}\mathbf{k}\cdot\hat{\mathbf{r}}}\mathrm{e}^{\mathrm{i}\mathbf{k}\cdot\mathbf{x}}\,\widehat{\mathbf{J}}(\mathbf{k})\frac{\mathrm{d}^3k}{(2\pi)^3}. \quad (22)$$

This expression is now inserted into eq. (21) and matrix elements of nuclear states and lattice states factorize. We denote $\mathbf{M}_{fi}^{(\mathrm{cms})}$ as the scattering matrix in the center of mass system and write

$$\begin{aligned}\mathbf{M}_{fi}(x,x') = \int &\langle\chi_f|\delta^3\big(\mathbf{y}-\hat{\mathbf{r}}(t)\big)\delta^3\big(\mathbf{y}'-\hat{\mathbf{r}}(t')\big)|\chi_i\rangle \\ &\times \mathbf{M}_{fi}^{(\mathrm{cms})}\big(\mathbf{x}-\mathbf{y},t;\mathbf{x}'-\mathbf{y}',t'\big)\,\mathrm{d}^3y\,\mathrm{d}^3y'. \end{aligned} \quad (23)$$

For $\hat{\mathbf{r}}=0$, one recovers the scattering matrix in the center of mass system, which we calculate in appendix A. The result is given by eq. (A.12), which we repeat in a more simple form:

$$\begin{aligned}\mathbf{M}_{fi}^{(\mathrm{cms})}(x,x') = &-\mathrm{i}\Theta(t-t')\mathrm{e}^{-\mathrm{i}\omega'_{fi}t}\mathrm{e}^{-(\mathrm{i}\omega_N+(\Gamma/2))(t-t')} \\ &\times\langle\phi_f|\,\hat{\mathbf{j}}(\mathbf{x})\widehat{U}_{\mathrm{hf}}(t-t')\hat{\mathbf{j}}(\mathbf{x}')\widehat{U}_{\mathrm{hf}}^{\dagger}(t-t')|\phi_i\rangle. \end{aligned} \quad (24)$$

The energy transfer to the nucleus is ω'_{fi} and Θ is the step function. ω_N and Γ are the transition energy and line width associated with a group of degenerate excited states.

[3] We define the Fourier transform of a function in space $f(\mathbf{x})$ by $\tilde{f}(\mathbf{k})=\int f(\mathbf{x})\exp(-\mathrm{i}\mathbf{k}\cdot\mathbf{x})\,\mathrm{d}^3x$. The inverse relationship is then $f(\mathbf{x})=\int\tilde{f}(\mathbf{k})\exp(\mathrm{i}\mathbf{k}\cdot\mathbf{x})\,\mathrm{d}^3k/(2\pi)^3$.

The time development operator $\widehat{U}_{\rm hf}(t) = \exp(-{\rm i}\widehat{H}_{\rm hf}t)$ exists due to static hyperfine interactions given by the Hamiltonian $\widehat{H}_{\rm hf}$. In this short form, we also assume that the nuclear current operators only facilitate transitions between any one of the (almost) degenerate ground states and excited states. A form of the scattering matrix that is useful for further calculations is now obtained by using space Fourier transforms of lattice and nuclear contributions:

$$\mathbf{M}_{fi}\big(x,x'\big) = -{\rm i}\Theta\big(t-t'\big)\,{\rm e}^{{\rm i}\omega_{fi}t}{\rm e}^{-({\rm i}\omega_N+(\Gamma/2))(t-t')} \times \int \mathcal{L}_{fi}\big(\mathbf{k},\mathbf{k}',t-t'\big)\,\mathbf{N}_{fi}\big(\mathbf{k},\mathbf{k}',t-t'\big)\,{\rm e}^{{\rm i}(\mathbf{k}\cdot\mathbf{x}+\mathbf{k}'\cdot\mathbf{x}')}\frac{{\rm d}^3k\,{\rm d}^3k'}{(2\pi)^6}. \quad (25)$$

Now ω_{fi} is the total energy difference, i.e., including lattice and nucleus, between final and initial states. The influence of vibrations is entirely contained in

$$\mathcal{L}_{fi}\big(\mathbf{k},\mathbf{k}',t\big) = \langle\chi_f|{\rm e}^{-{\rm i}\mathbf{k}\cdot\hat{\mathbf{r}}}\widehat{U}_L(t){\rm e}^{-{\rm i}\mathbf{k}'\cdot\hat{\mathbf{r}}}\widehat{U}_L^\dagger(t)|\chi_i\rangle. \quad (26)$$

The spectrum of $\mathcal{L}$ consists of all possible vibrational lattice excitations and has a typical energy spread of less than ±1 eV. The matrix elements of the nuclear currents are

$$\mathbf{N}_{fi}\big(\mathbf{k},\mathbf{k}',t\big) = \langle\phi_f|\,\widehat{\mathbf{J}}(\mathbf{k})\widehat{U}_{\rm hf}(t)\widehat{\mathbf{J}}\big(\mathbf{k}'\big)\widehat{U}_{\rm hf}^\dagger(t)|\phi_i\rangle. \quad (27)$$

Using this expression, we must remember that only sublevels associated with a particular nuclear transition can be considered. The spectrum of $\mathbf{N}$ is determined by the nuclear level splitting caused by hyperfine interactions. Without hyperfine interactions, $\mathbf{N}$ is independent of time.

If the vector potential of the incident radiation, $\mathbf{A}_0$, is given, the scattered vector potential follows from eqs. (12) and (25). Therefore, we need reasonable assumptions about the vector potential of the incident radiation. A case of particular interest occurs for monochromatized synchrotron radiation (SR). The X-rays emitted by the present SR sources can be understood as an incoherent superposition of one-photon fields. This does not change by monochromatization, and the individual one-photon fields henceforth will be called "SR components". It is then safe to apply our formalism to each SR component and perform an incoherent average over their individual properties, i.e., when calculating intensities. For each SR component, the coherence length for all directions in space is much larger than the size of the nucleus. This is caused by a large distance between nucleus and SR source, as well as by the monochromatization process. The incident field may then be represented by a plane quasimonochromatic wave with wave vector $\mathbf{k}_0$, average energy $\omega_0 = |\mathbf{k}_0|$, and a time-dependent amplitude, i.e., $\mathbf{A}_0(x) = \mathbf{p}a(t)\exp({\rm i}\mathbf{k}_0\cdot\mathbf{x} - {\rm i}\omega_0 t)$. The unit vector $\mathbf{p}$ gives the time-independent polarization of the SR component. The function $a(t)$ describes the pulse structure of the SR component, as well as its energy spectrum including the modification by a monochromator. We assume that $a(t) = 0$ outside the time interval $[t_0, t_0 + \delta t]$, i.e., the SR component arrives at time t_0 at the nucleus and has a duration δt. The duration shall be much smaller than the nuclear lifetime and the inverse of the typical nuclear

level splitting. The set $\{\mathbf{k}_0, \mathbf{p}, a(t)\}$ presents a unique description of the SR component. If eq. (14) is used, one obtains the expression $\omega_0|a|^2/(4\pi)$ for the probability per unit time and area to observe the photon from a particular SR component at the location of the nucleus. The scattered vector potential is calculated from eq. (12) by integrating the poles of δ_+ and using the Fourier-transformed scattering matrix. At sufficiently large distances from the nucleus at $\mathbf{x} = 0$ one obtains

$$\mathbf{A}_{fi}(x) = -\mathrm{i}\frac{\mathrm{e}^{-\mathrm{i}(\omega_0-\omega_{fi})t_\mathrm{r}}}{|\mathbf{x}|}\int_0^\infty \mathrm{e}^{-(\Gamma/2)t'}\mathrm{e}^{\mathrm{i}(\omega_0-\omega_N)t'}\mathcal{L}_{fi}\big(-\mathbf{k}_S, \mathbf{k}_0, t'\big) \times \mathbf{N}_{fi}\big(-\mathbf{k}_S, \mathbf{k}_0, t'\big)\mathbf{p}a\big(t_\mathrm{r} - t'\big)\,\mathrm{d}t', \tag{28}$$

where the retarded time $t_\mathrm{r} = t - |\mathbf{x}|$ and the wave vector $\mathbf{k}_S = (\omega_0 - \omega_{fi})\,\mathbf{x}/|\mathbf{x}|$ were introduced. Clearly eq. (28) describes a spherical wave with time-dependent amplitude emanating from the nucleus. Taking into account the time properties of $a(t)$ given by the pulse structure of the SR component, one sees that, in fact, the integration in eq. (28) is carried out from $t' = t_\mathrm{r} - t_0$ to $t' = t_\mathrm{r} - t_0 + \delta t$. In this interval we may neglect the time dependence of the function $\mathbf{N}(t)\exp(-\Gamma t/2)$ and write

$$\mathbf{A}_{fi}(x) = -\mathrm{i}\Theta(t_\mathrm{r} - t_0)\frac{\mathrm{e}^{-\mathrm{i}(\omega_0-\omega_{fi})t_\mathrm{r}}}{|\mathbf{x}|}\mathrm{e}^{-(\Gamma/2)(t_\mathrm{r}-t_0)}\mathbf{N}_{fi}(-\mathbf{k}_S, \mathbf{k}_0, t_\mathrm{r} - t_0)\mathbf{p} \times \int \mathcal{L}_{fi}\big(-\mathbf{k}_S, \mathbf{k}_0, t'\big)\mathrm{e}^{\mathrm{i}(\omega_0-\omega_N)t'}a\big(t_\mathrm{r} - t'\big)\,\mathrm{d}t. \tag{29}$$

The scattered vector potential following from this expression is inserted into eq. (14) to provide the probability per time and solid angle to observe the scattered photon. Also the quantum state of the scatterer changes from $|\chi_i\rangle|\phi_i\rangle$ to $|\chi_f\rangle|\phi_f\rangle$. As pointed out earlier, initial and final states of the nucleus must differ, i.e., $|\phi_f\rangle \neq |\phi_i\rangle$. In scattering experiments, the initial and final states of the scatterer are usually not known. We accommodate this situation by an average over initial states and a restricted sum over final states:

$$\frac{\mathrm{d}^2P}{\mathrm{d}\Omega\,\mathrm{d}t} = \left\langle \sum_f \frac{\mathrm{d}^2P_{fi}}{\mathrm{d}\Omega\,\mathrm{d}t}\right\rangle = \frac{\omega_0}{4\pi}|\mathbf{x}|^2\left\langle \sum_f |\mathbf{A}_{fi}|^2\right\rangle. \tag{30}$$

The angular brackets symbolize averaging over initial states. After inserting the scattered potential from eq. (29), a clearly arranged expression is obtained:

$$\frac{\mathrm{d}^2P}{\mathrm{d}\Omega\,\mathrm{d}t} = \frac{\pi}{2}\frac{\sigma\Gamma}{1+\alpha}\Theta(t)\Gamma\mathrm{e}^{-\Gamma t}N(\mathbf{k}_S, \mathbf{k}_0, t) \times \frac{\omega_0}{2(2\pi)^2}\int \widetilde{L}(\mathbf{k}_0, \omega + \omega_0 - \omega_N)\big|\tilde{a}(\omega)\big|^2\frac{\mathrm{d}\omega}{2\pi}. \tag{31}$$

For clarity $(t_\mathrm{r} - t_0)$ was replaced with t; σ and α are the nuclear resonant cross-section and the internal conversion coefficient, respectively. The function $\tilde{a}$ is the time Fourier

transform[4] of the pulse structure of the SR component. The time-dependent angular correlation function is defined by

$$N(\mathbf{k}_S, \mathbf{k}_0, t) = \frac{4(1+\alpha)}{\sigma\Gamma^2}\left\langle \sum_{f\neq i} |\mathbf{N}_{fi}(-\mathbf{k}_S, \mathbf{k}_0, t)\mathbf{p}|^2 \right\rangle. \tag{32}$$

The factor is chosen to normalize N with respect to integration over all directions of the emitted photon if the restriction $f \neq i$ is abandoned. This is permissible for the special case of a single nucleus. Nuclear resonant fluorescence from an ensemble of nuclei always gives $\int N \,\mathrm{d}\Omega < 1$. The calculation is presented in appendix B. $\widetilde{L}$ is the Fourier image of the vibrational self-intermediate scattering function of the nucleus, which is given by

$$\begin{aligned} L(\mathbf{k}_0, t) &= \left\langle \sum_f \mathcal{L}_{fi}{}^*\big(-\mathbf{k}_S, \mathbf{k}_0, t+t'\big)\mathcal{L}_{fi}\big(-\mathbf{k}_S, \mathbf{k}_0, t'\big) \right\rangle \\ &= \left\langle \mathrm{e}^{\mathrm{i}\mathbf{k}_0\cdot\hat{\mathbf{r}}(t)}\mathrm{e}^{-\mathrm{i}\mathbf{k}_0\cdot\hat{\mathbf{r}}(0)} \right\rangle. \end{aligned} \tag{33}$$

In this case, the sum over final states $|\chi_f\rangle$ is unrestricted, and closure in combination with the unitarity of the operator $\exp(\mathrm{i}\mathbf{k}_S \cdot \hat{\mathbf{r}})$ permits significant simplification. We note that the vibrational self-intermediate scattering function is independent of the wave vector $\mathbf{k}_S$ of the scattered photon and thus independent of the momentum transfer $\mathbf{k}_S - \mathbf{k}_0$ to the scatterer. The self-intermediate scattering function is normalized to unity at $t = 0$, i.e., $L(\mathbf{k}, 0) = 1$ and therefore $\int \widetilde{L}(\mathbf{k}, \omega)\,\mathrm{d}\omega = 2\pi$. Equation (31) describes the scattering of an individual SR component. The full description is obtained after averaging this equation over all SR components, i.e., over all relevant sets $\{\mathbf{k}_0, \mathbf{p}, a(t)\}$. For a SR pulse, the fluctuation in the arrival times t_0 and polarizations $\mathbf{p}$ can be neglected. Thus, only the integral in eq. (31) has to be averaged, and we obtain the result

$$\frac{\mathrm{d}^2 P}{\mathrm{d}\Omega\,\mathrm{d}t} = \frac{\pi}{2}\frac{\sigma\Gamma}{1+\alpha}\Theta(t)\Gamma\mathrm{e}^{-\Gamma t}N(\mathbf{k}_S, \mathbf{k}_0, t)\int \widetilde{L}(\mathbf{k}_0, \omega-\omega_N)I(\omega)\frac{\mathrm{d}\omega}{2\pi}, \tag{34}$$

where $I(\omega)$ gives the average probability per unit energy and area to find a photon with energy ω incident on the nucleus. We write explicitly

$$I(\omega) = \overline{\frac{\omega_0}{2(2\pi)^2}\big|\tilde{a}(\omega+\omega_0)\big|^2}. \tag{35}$$

The shape of $I(\omega)$ can be identified with the resolution function of the monochromator.

Equation (34) quantifies the relationship between nuclear resonant fluorescence and the spectrum of atomic vibrations. It describes an exponential decay with the lifetime of the excited nuclear state $\tau = 1/\Gamma$ that is modulated by oscillations originating in the hyperfine splitting of the nuclear states. The integral in eq. (34) essentially

[4] We define the Fourier transform of a function in time $f(t)$ by $\tilde{f}(\omega) = \int f(t)\exp(\mathrm{i}\,\omega t)\,\mathrm{d}t$. The inverse relationship is then $f(t) = \int \tilde{f}(\omega)\exp(-\mathrm{i}\omega t)\,\mathrm{d}\omega/(2\pi)$.

convolutes the monochromator resolution function with the spectrum of vibrational excitations. It directly follows from eq. (34) that $\widetilde{L}$ and thus the vibrational self-intermediate scattering function can in principle be determined from nuclear resonant fluorescence independent of time of observation and direction of emission of the fluorescence photon. We are therefore provided with a recipe for experiments. The energy of sufficiently monochromatized pulsed synchrotron radiation is tuned with respect to the nuclear transition energy. The intensity of the incoherently scattered radiation from a sample that occurs with time delay is measured. To accommodate this situation, eq. (34) is integrated over a certain time interval $[t_1, t_2]$ and several directions of the emitted radiation. We also introduce the centered and normalized resolution function of the monochromator $R(\omega) = I(\omega - \overline{\omega})/I_0$ with center energy $\overline{\omega} = \int \omega I(\omega)\,\mathrm{d}\omega/I_0$ and normalization constant $I_0 = \int I(\omega)\,\mathrm{d}\omega$. This results in

$$P_{\mathrm{exp}}(\Delta\omega, t_1, t_2) = I_0 \frac{\pi}{2} \frac{\sigma\Gamma}{1+\alpha} W(\mathbf{k}_0, t_1, t_2) \int \widetilde{L}(\mathbf{k}_0, \omega + \Delta\omega) R(\omega) \frac{\mathrm{d}\omega}{2\pi}, \qquad (36)$$

where $\Delta\omega = \overline{\omega} - \omega_N$ is the energy transfer to the lattice and I_0 is the probability per unit area for photons to be incident on the nucleus. The weight W depends on the particular integration intervals and the direction of the incident photon. We can derive W from eqs. (32) and (34):

$$W(\mathbf{k}_0, t_1, t_2) = \Gamma \int_{t_1}^{t_2} \mathrm{d}t \int_{\Omega_S} \mathrm{d}\Omega\, \mathrm{e}^{-\Gamma t} N(\mathbf{k}_S, \mathbf{k}_0, t). \qquad (37)$$

The calculations in appendix B show that we always have $W < 1$ unless the integrations are complete and the restriction $f \neq i$ is abandoned, i.e., we consider a single nucleus. In the latter case, one obtains $W = 1$, giving the maximum number of photons that can be emitted by an individual nucleus via the scattering channel discussed in this section.

3.2. Atomic fluorescence following nuclear absorption

The mechanism for the calculation of the intensity of atomic fluorescence radiation is virtually identical to that in the previous section. The scattering matrix according to the diagram in figure 2(c) is calculated in appendix C. It appears in completely analogous form to eq. (25) with the matrix $\mathbf{N}$ replaced by

$$\mathbf{N}'_{fi}(\mathbf{k}, \mathbf{k}', t) = \langle \phi_f | \widehat{\mathbf{S}}(\mathbf{k}) \widehat{B} \widehat{U}_{\mathrm{hf}}(t) \widehat{\mathbf{J}}(\mathbf{k}') \widehat{U}^{\dagger}_{\mathrm{hf}}(t) | \phi_i \rangle, \qquad (38)$$

where $\widehat{\mathbf{S}}(\mathbf{k})$ is the spatial Fourier transform of the transverse electronic current $\hat{\mathbf{s}}(\mathbf{x}, t)$ at $t = 0$. Whereas in eq. (25) a transverse nuclear current is the source of the emitted photon, now the transverse electronic current $\widehat{\mathbf{S}}(\mathbf{k})\widehat{B}$ serves as the source for the fluorescence photon. Although the formal similarity of eqs. (38) and (25) is obvious, we have to remember that the properties of the emitted fluorescence photon

will depend on nuclear as well as electronic properties, i.e., the states $|\phi\rangle$ characterize the whole ion core. The operator $\widehat{B}$ is calculated in appendix C and is given by

$$\widehat{B} = \int \Theta(t')\,\mathrm{e}^{-(\hat{\Delta}-\mathrm{i}\omega_N)\,t'}\widehat{U}_N(t')\,\hat{s}_\mu(\mathbf{y})\widehat{U}_N^\dagger(t')\hat{j}_\mu(\mathbf{y}') \times \frac{\cos\omega_N|\mathbf{y}-\mathbf{y}'|}{|\mathbf{y}-\mathbf{y}'|}\,\mathrm{d}^3y\,\mathrm{d}^3y'\,\mathrm{d}t'. \tag{39}$$

The time development operator $\widehat{U}_N(t) = \exp(-\mathrm{i}\widehat{H}_N t)$ is given by the Hamiltonian $\widehat{H}_N$ that according to eq. (16) describes the ion core. The term depending on the spatial distance of the two vertices at $\mathbf{y}$ and $\mathbf{y}'$ represents a standing spherical wave with wavelength $2\pi/\omega_N$. It arises from the exchange of virtual photons (horizontal wavy line in figure 2(c)) with energy ω_N. The level shift operator $\widehat{\Delta}$ produces the energy width of the excited electronic state (atom with a core hole), which is symbolized in figure 2(c) by the right double line. The calculation of the scattered photon field, now representing fluorescence radiation, proceeds analogously to the previous section. The number of emitted fluorescence photons per time and solid angle is

$$\frac{\mathrm{d}^2P}{\mathrm{d}\Omega\,\mathrm{d}t} = \frac{\pi}{2}\frac{\alpha\eta\sigma\Gamma}{1+\alpha}\Theta(t)\Gamma\mathrm{e}^{-\Gamma t}N'(\mathbf{k}_S,\mathbf{k}_0,t)\int \widetilde{L}(\mathbf{k}_0,\omega-\omega_N)I(\omega)\frac{\mathrm{d}\omega}{2\pi}, \tag{40}$$

where the time-dependent angular correlation is now derived from eq. (38) and calculated as

$$N'(\mathbf{k}_S,\mathbf{k}_0,t) = \frac{4(1+\alpha)k_0}{\alpha\eta\sigma\Gamma^2 k_S}\left\langle \sum_f \left|\mathbf{N}'_{fi}(-\mathbf{k}_S,\mathbf{k}_0,t)\mathbf{p}\right|^2\right\rangle. \tag{41}$$

Contrary to our calculation of nuclear resonant fluorescence, we no longer have to maintain the restriction $|\phi_f\rangle \neq |\phi_i\rangle$ in the sum over final states, because, in fact, the scattering matrix elements vanish for $|\phi_f\rangle = |\phi_i\rangle$. The factor is chosen to maintain the normalization $\int N'\,\mathrm{d}\Omega = 1$. $\eta < 1$ is known as the fluorescence yield. As before, we integrate eq. (40) over a certain time interval and several directions of the emitted radiation, resulting in

$$P_{\mathrm{exp}}(\Delta\omega,t_1,t_2) = I_0\frac{\pi}{2}\frac{\alpha\eta\sigma\Gamma}{1+\alpha}W'(\mathbf{k}_0,t_1,t_2)\int \widetilde{L}(\mathbf{k}_0,\omega+\Delta\omega)R(\omega)\frac{\mathrm{d}\omega}{2\pi}. \tag{42}$$

The weight W' is expressed in analogy to eq. (37) as

$$W'(\mathbf{k}_0,t_1,t_2) = \Gamma\int_{t_1}^{t_2}\mathrm{d}t\int_{\Omega_S}\mathrm{d}\Omega\,\mathrm{e}^{-\Gamma t}N'(\mathbf{k}_S,\mathbf{k}_0,t). \tag{43}$$

If the integration over directions of the emitted radiation is complete, the normalization condition for N' leads to $W' = (\exp(-\Gamma t_1) - \exp(-\Gamma t_2)) < 1$, which is independent of $\mathbf{k}_0$. If the time integration is also complete, one obtains $W' = 1$, giving the maximum number of photons that can be emitted by an individual nucleus via atomic fluorescence, the scattering channel discussed in this section.

The final results that were obtained for the two discussed channels of incoherent nuclear resonant scattering are very similar. Both eqs. (36) and (42) show the same dependence on the spectrum of atomic vibrations. The two incoherent scattering channels are equivalent in this respect. In experimental applications, the second method is often preferred, mostly for practical reasons [14].

4. Macroscopic samples

In the previous section, incoherent scattering contributions from individual nuclei within an ensemble were calculated. Measurements usually require a large number of atoms. A coarse estimate for the number of nuclei required to produce a reasonable NRS signal is, e.g., obtained from the completely integrated version of eq. (42) assuming broad-band incident radiation. The number of scattered photons from n nuclei is then $P = n\pi\sigma\eta\Gamma I_0/(2(1+\alpha))$. Today's X-ray sources provide $I_0 \approx 10^{12}$ Hz/(eV mm^2) onto the sample. With the parameters of the 14.4 keV transition of ^{57}Fe, we find $P \approx 5n \cdot 10^{-13}$ Hz, which implies values $n > 10^{15}$. The need for macroscopic samples requires a study of other X-ray scattering channels in condensed matter and, in particular, any interplay with coherent NRS. Following the classification scheme of figure 1, one can identify six important X-ray scattering channels, coherent elastic nuclear resonant scattering (CENRS), coherent inelastic nuclear resonant scattering (CINRS), incoherent nuclear resonant scattering (INRS), coherent elastic electronic scattering (CEES), coherent inelastic electronic scattering (CIES), and incoherent electronic scattering (IES).[5]

In figure 3, several relevant situations are displayed. Each hexagon in the figure symbolizes a compact tree level schematic in the following sense. One chooses a cornerpoint as the origin of the tree level diagram. The remaining five cornerpoints correspond to five branches leading to the next level. The selection of the branch is indicated by an arrow, thereby defining a new cornerpoint, and the whole procedure is repeated. Panel (a) shows dominant channels if the incident radiation can excite the nuclear resonance directly. The interplay of coherent and incoherent channels has been investigated by Baron et al. [19] and Sturhahn et al. [20]. In investigations of lattice vibrations, a reduction of the incoherently scattered intensity in the "elastic peak" was reported by Sturhahn et al. [12]. If the incident radiation is tuned off resonance, INRS remains as the dominant scattering channel. Less important terms are symbolized by panel (b). Calculations indicate that CINRS contributions should always be small [32]. This result follows from a combination of two effects. First, in a thermalized ensemble the lifetime of the vibrational states is short compared to the nuclear lifetime. This argument was used earlier by Chumakov et al. [13] to explain the smallness of CINRS. However, this is not sufficient, as the following argument shows [33]. The relevant

[5] Scattering channels related to the electronic–nuclear interference terms were neglected.

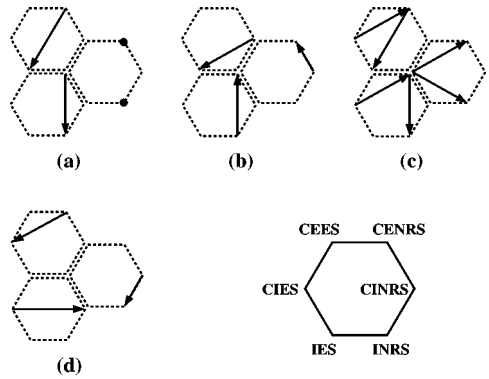

Figure 3. Schematic of X-ray scattering processes in macroscopic samples. As shown in the lower right, the cornerpoints of each hexagon symbolize X-ray scattering channels, coherent elastic nuclear resonant scattering (CENRS), coherent inelastic nuclear resonant scattering (CINRS), incoherent nuclear resonant scattering (INRS), coherent elastic electronic scattering (CEES), coherent inelastic electronic scattering (CIES), and incoherent electronic scattering (IES.) Arrows between cornerpoints stand for a combination of scattering channels, e.g., in panel (a) the upper left hexagon depicts coherent elastic nuclear resonant scattering followed by electronic absorption or Compton scattering. The hexagon can be understood as a compactification of a tree level schematic, where branches are now arrows between cornerpoints. Each panel shows a class of scattering processes involving NRS: direct excitation of the nuclear resonance in panel (a), less important terms in off-resonance excitation of the nuclear resonance in panel (b), leading contamination of INRS by inelastic scattering from electrons in panel (c); examples of negligible higher order terms are shown in panel (d).

matrix elements for CINRS are proportional to

$$\left\langle \sum_f \mathcal{L}_{fi}^{(j)*}\big(\mathbf{k},\mathbf{k}',t\big)\mathcal{L}_{fi}^{(j')}\big(\mathbf{k},\mathbf{k}',t'\big)\right\rangle, \tag{44}$$

where j, j' indicate nuclei of the ensemble and $\mathcal{L}$ is taken from eq. (26). A closer look shows that the lifetime argument does not apply to all terms in the sum and, with the assumption that the ensemble is excited off resonance, the following terms remain:

$$\sum_{fi} w_i \langle\chi_i|\mathrm{e}^{-\mathrm{i}\mathbf{k}'\cdot\hat{\mathbf{r}}_j(-t)}|\chi_f\rangle\langle\chi_f|\mathrm{e}^{\mathrm{i}\mathbf{k}\cdot\hat{\mathbf{r}}_j}|\chi_f\rangle\langle\chi_f|\mathrm{e}^{-\mathrm{i}\mathbf{k}\cdot\hat{\mathbf{r}}_{j'}}|\chi_f\rangle\langle\chi_f|\mathrm{e}^{\mathrm{i}\mathbf{k}'\cdot\hat{\mathbf{r}}_{j'}(-t')}|\chi_i\rangle. \tag{45}$$

This contribution to CINRS originates from the creation of a phonon during absorption of the incident photon whereas during re-emission the lattice state remains unchanged. The term is not negligible but of the order L times the Lamb–Mössbauer factor. The second effect that eventually causes CINRS to be small originates in the energy of the emitted photon. Because the lattice state does not change during re-emission, the energy of the scattered photon exactly matches the nuclear transition energy. This leads to strong absorption of the narrow-bandwidth scattered radiation by CENRS, and only a small fraction of the ensemble may actually contribute to a measurable intensity.

Chumakov et al. [29] observed that nuclear resonant fluorescence followed by CENRS leads to radiation trapping inside the sample, and the decay time of the emitted

radiation is enlarged. The resulting additional factor in eq. (36) is independent of the energy transfer to the lattice vibrations. The terms that are shown in panel (c) involve CIES, which can complicate the dependence on lattice properties. One can show, however, that these contributions do not exceed 10^{-3} of the dominant INRS channel [34]. Finally, a few of the many possibilities of higher order multiple scattering terms are indicated in panel (d). Their magnitude is negligible.

The smallness of the contributions in figure 3(c) precludes any effects from vibrations of nonresonant nuclei on the time dependence or yield of INRS. Because CINRS is weak, we conclude that the self-intermediate scattering function of the nuclear motion, defined by eq. (33), describes the relationship between NRS and lattice vibrations in macroscopic samples. It is a unique feature of INRS to provide local vibrational properties.

5. Lattice dynamics and NRS

Incoherent NRS is connected with the local lattice dynamics via the self-intermediate scattering function defined in eq. (33). The dynamics of the displacement operator is determined by the Hamiltonian $\widehat{H} = \widehat{H}_L + \widehat{H}_E + \widehat{V}$, where the Hamiltonians on the right are those from eq. (16). For a lattice in thermal equilibrium, the self-intermediate scattering function takes the form

$$L_j(\mathbf{k}, t) = \frac{\mathrm{Trace}\{\mathrm{e}^{-\beta\widehat{H}}\mathrm{e}^{\mathrm{i}\mathbf{k}\cdot\hat{\mathbf{r}}_j(t)}\mathrm{e}^{-\mathrm{i}\mathbf{k}\cdot\hat{\mathbf{r}}_j(0)}\}}{\mathrm{Trace}\{\mathrm{e}^{-\beta\widehat{H}}\}}, \tag{46}$$

where β is the inverse temperature, and the local character of the self-intermediate scattering function is expressed by the index j. The trace is taken with respect to a complete set of quantum numbers describing the eigenstates of the Hamiltonian $\widehat{H}$. Using cyclic permutations of the trace operation and parity conservation by the Hamiltonian, which is constructed from electromagnetic interactions, an important symmetry property of $L(\mathbf{k}, t)$ and its Fourier transform is derived:

$$L(\mathbf{k}, t) = L(\mathbf{k}, -t - \mathrm{i}\,\beta), \qquad \widetilde{L}(\mathbf{k}, \omega) = \mathrm{e}^{\beta\omega}\widetilde{L}(\mathbf{k}, -\omega). \tag{47}$$

The spectrum of the self-intermediate scattering function $\widetilde{L}$ exhibits a detailed balance. The time derivatives of L are related to the moments of $\widetilde{L}$ by virtue of the Fourier transformation. The lowest order moments can be calculated under quite general circumstances and form Lipkin's sum rules [35,36]. Obviously the moments convey information about the short-term dynamics of the vibrations. Assume one knows a complete set of eigenstates given by $\{|\chi_n\rangle\}$ with energies ε_n. Equation (46) can then be expressed as a superposition of simple exponentials:

$$L(\mathbf{k}, t) = \sum_{ni} p_i \left|\langle\chi_n|\mathrm{e}^{-\mathrm{i}\mathbf{k}\cdot\hat{\mathbf{r}}}|\chi_i\rangle\right|^2 \mathrm{e}^{\mathrm{i}\varepsilon_{ni}t}, \tag{48}$$

where $p_i = \exp(-\beta\varepsilon_i)/Z$ with $Z = \sum_i \exp(-\beta\varepsilon_i)$ is the normalized Boltzmann factor. Exact "a priori" eigenstates and excitation energies of many-body systems are not known, and one has to adopt models that can be solved. In many cases, it will be possible to split the Hamiltonian into several, commuting contributions, i.e., $\widehat{H} = \sum_j \widehat{H}_j$ and $[\widehat{H}_j, \widehat{H}_{j'}] = 0$. Any of the terms that commutes with $\hat{\mathbf{r}}$ does not contribute to the dynamics of the atomic position and need not be considered in the calculation of the self-intermediate scattering function. In our derivation, we considered vibrations but excluded rotational excitations. Two examples that can be treated under these circumstances are the ideal gas and the harmonic lattice. Both cases will be discussed in more detail below.

5.1. The ideal gas

The ideal gas is an ensemble of noninteracting atoms. This case was discussed earlier; Van Hove [22] calculated the self-correlation function, Singwi and Sjölander [5] studied the self-intermediate scattering function. The nonrelativistic Hamiltonian of an ideal monoatomic gas, i.e., without rotational degrees of freedom, is the sum of the kinetic energies of the individual atoms:

$$\widehat{H} = \sum_j \frac{\hat{\mathbf{p}}_j^2}{2m_j}. \tag{49}$$

It is clear that the self-intermediate scattering function can be calculated with one term in the sum only, and we omit the index j. Using $a = -\beta/(2m)$ and $b = -\mathrm{i}t/(2m)$, we obtain

$$L(\mathbf{k}, t) = \frac{\mathrm{Trace}\{\mathrm{e}^{(a-b)\hat{\mathbf{p}}^2}\,\mathrm{e}^{\mathrm{i}\mathbf{k}\cdot\hat{\mathbf{r}}(0)}\mathrm{e}^{b\hat{\mathbf{p}}^2}\mathrm{e}^{-\mathrm{i}\mathbf{k}\cdot\hat{\mathbf{r}}(0)}\}}{\mathrm{Trace}\{\mathrm{e}^{a\hat{\mathbf{p}}^2}\}}. \tag{50}$$

The usual commutation rules for momentum and position operators permit us to calculate the commutator of the exponentials in the previous expression, e.g.,

$$\mathrm{e}^{b\hat{\mathbf{p}}^2}\mathrm{e}^{-\mathrm{i}\mathbf{k}\cdot\hat{\mathbf{r}}} = \mathrm{e}^{-\mathrm{i}\mathbf{k}\cdot\hat{\mathbf{r}}}\,\mathrm{e}^{b(\hat{\mathbf{p}}-\mathbf{k})^2}. \tag{51}$$

After some manipulation we obtain the result

$$L(k, t) = \exp\left(-\mathrm{i}\omega_\mathrm{R}t - \frac{\omega_\mathrm{R}}{\beta}t^2\right), \tag{52}$$

where $\omega_\mathrm{R} = k^2/(2m)$ is the recoil energy. The Fourier transform is also easily calculated:

$$\widetilde{L}(k, \omega) = \sqrt{\frac{\pi\beta}{\omega_\mathrm{R}}}\exp\left(-\frac{\beta}{4\omega_\mathrm{R}}(\omega - \omega_\mathrm{R})^2\right). \tag{53}$$

As expected, we obtain a Gaussian centered around the recoil energy with a width proportional to the square root of temperature and recoil energy.

5.2. The harmonic lattice

The dynamic behavior of atoms bound in a solid is, for small vibrational amplitudes, well described by the harmonic lattice model. Background and physical relevance of this model are discussed in several textbooks, e.g., Ashcroft and Mermin [37]. Recently Kohn et al. [38] analyzed nuclear resonant absorption in anisotropic single crystals using the harmonic lattice model. The harmonic lattice is also frequently used to model materials with randomly arranged atoms [39,40]. Here we do not require translational symmetries of the lattice, and our treatment is suitable for crystals as well as disordered or amorphous materials. The Hamiltonian for the harmonic lattice is

$$\widehat{H} = \sum_j \frac{\hat{\mathbf{p}}_j^2}{2m_j} + \frac{1}{2}\sum_{jj'} \hat{\mathbf{u}}_j \mathbf{D}_{jj'} \hat{\mathbf{u}}_{j'}, \tag{54}$$

where $\hat{\mathbf{p}}_j$ are the momenta of the atoms, m_j are the masses of the atoms, $\hat{\mathbf{u}}_j$ are the displacements of the atoms with respect to their average positions. The force constant matrix $\mathbf{D}_{jj'}$ is real, symmetric, and independent of time. If no forces act on the center of mass of the solid, we have $\sum_j \mathbf{D}_{jj'} = 0$, which means $\mathbf{D}_{jj'}$ is singular, i.e., at least one eigenvalue is zero. This poses a slight problem because it leads to the occurrence of zero-energy excitations. This can be avoided by reformulating the Hamiltonian in the center of mass system of the solid. We define $\widehat{\mathbf{P}} = \sum_j \hat{\mathbf{p}}_j$ and $\widehat{\mathbf{R}} = \sum_j m_j \hat{\mathbf{u}}_j / M$ with $M = \sum_j m_j \gg m_j$ as the dynamic variables of the center of mass and remove a pair of atomic variables from the sums in eq. (54). One also introduces particle creation and annihilation operators $\hat{a}_l$, $\hat{a}_l^\dagger$ (see, e.g., [41]). In cases with translational symmetries of the lattice, e.g., single crystals, these particles are delocalized and they are called phonons. From the calculations in appendix D we carry over

$$\widehat{H} = \frac{\widehat{\mathbf{P}}^2}{2M} + \sum_l \omega_l \left(\hat{a}_l^\dagger \hat{a}_l + \frac{1}{2} \right). \tag{55}$$

The sum runs over all translational degrees of freedom and $\omega_l > 0$ are the particle energies.[6] The self-intermediate scattering function is now calculated as a product of the contributions of each particle mode and a factor for the center of mass motion:

$$L_j(\mathbf{k}, t) = L_{\text{cms}}(k, t) \prod_l L_{jl}(\mathbf{k}, t). \tag{56}$$

The first factor is formally identical to eq. (52), but the recoil energy has to be calculated with the total mass of the solid.[7] The factors from the particle modes are calculated

[6] To avoid confusion we will use indices l, l' to enumerate degrees of freedom or particle modes and indices j, j' to enumerate atoms of the ensemble.

[7] The condition for "recoilless" NRS or Mössbauer absorption $\omega_R < \Gamma$ leads to a minimum allowed mass for the solid. For the 14.4 keV transition of the Mössbauer isotope ^{57}Fe, one obtains $M > 2.4 \cdot 10^7$ atomic mass units.

in appendix D. They are given by

$$L_{jl}(\mathbf{k},t) = \exp\{-|\alpha_{jl}|^2\big(1 - \mathrm{e}^{-\mathrm{i}\omega_l t} + n_l\big|1 - \mathrm{e}^{-\mathrm{i}\omega_l t}\big|^2\big)\}, \quad \alpha_{jl} = \frac{\mathrm{i}\mathbf{k}\cdot\mathbf{X}^*_{jl}}{\sqrt{2m_j\omega_l}}, \tag{57}$$

where the occupation numbers in thermal equilibrium are $n_l = 1/(\exp(\beta\omega_l) - 1)$. For large ensembles or sufficiently low temperatures, the number of excited particles per atom is a very small number, i.e., $|\alpha_{jl}|^2 n_l \ll 1$. After combining the contributions of the individual particle modes, we obtain for the self-intermediate scattering function of the harmonic lattice

$$L_j(\mathbf{k},t) = L_{\mathrm{cms}}(k,t) \times \exp\left\{-\int \frac{\omega_\mathrm{R}}{\omega}\, g_j(\mathbf{s},\omega)\big((1+n_\omega)\big(1-\mathrm{e}^{-\mathrm{i}\omega t}\big) + n_\omega\big(1-\mathrm{e}^{\mathrm{i}\omega t}\big)\big)\,\mathrm{d}\omega\right\}, \tag{58}$$

where $\omega_\mathrm{R} = k^2/(2m_j)$ is the recoil energy of the free atom and $n_\omega = 1/(\exp(\beta\omega) - 1)$. The function g_j has the character of a local particle density of states (DOS) that also depends on the direction $\mathbf{s}$ of the photon incident on the resonant isotope. It is defined by the symmetric quadratic form

$$g_j(\mathbf{s},\omega) = \mathbf{s}\left(\sum_l \mathbf{X}_{jl}\,\mathbf{X}^\dagger_{lj}\delta(\omega-\omega_l)\right)\mathbf{s}. \tag{59}$$

This expression generalizes the results of Kohn et al. [38], which were obtained for anisotropic single crystals, to an arbitrary system with harmonic interactions. Using the unitarity of the eigenvector matrices, one can easily show that $\int g_j(\mathbf{s},\omega)\,\mathrm{d}\omega = 1$. In eq. (59), the expression in parentheses is a second rank tensor in ordinary space, which can always be decomposed into a trace, an antisymmetric part, and a traceless symmetric part [42]. Under rotations in space, the trace is invariant. The antisymmetric part does not contribute to the quadratic form, and the traceless symmetric part transforms like a second rank irreducible tensor. It is then quite useful to write

$$g_j(\mathbf{s},\omega) = \frac{1}{3}\mathcal{D}_j(\omega) + \mathcal{A}_j(\mathbf{s},\omega), \quad \mathcal{D}_j(\omega) = \mathrm{Trace}\left\{\sum_l \mathbf{X}_{jl}\,\mathbf{X}^\dagger_{lj}\delta(\omega-\omega_l)\right\}, \tag{60}$$

where $\mathcal{D}_j$ is the local DOS and the anisotropic vibrational behavior is contained in $\mathcal{A}_j$. By definition, $\int \mathcal{D}_j(\omega)\,\mathrm{d}\omega = 3$ and $\int \mathcal{A}_j(\mathbf{s},\omega)\,\mathrm{d}\omega = 0$, as well as $\int \mathcal{A}_j(\mathbf{s},\omega)\,\mathrm{d}^2 s = 0$. The rotational symmetries of the system determine the general form of the anisotropic part. For crystalline systems, the traceless symmetric tensor used to construct the quadratic form $\mathcal{A}_j$ is isomorphic to the traceless part of the metric tensor [43]. Let the angles θ, φ give the direction of the incident radiation in the main axes system of the metric tensor. Then we may write

$$\mathcal{A}_j(\mathbf{s},\omega) = \mathcal{A}^{(p)}_j(\omega)Y_{20}(\theta,\varphi) + \mathcal{A}^{(a)}_j(\omega)\Re\{Y_{22}(\theta,\varphi)\}, \tag{61}$$

Table 1
Vibrational anisotropies in Bravais lattices. The polar and azimuthal anisotropies are defined in eq. (61). Even if the crystal symmetry does not require anisotropies to vanish, they can still be zero for other reasons.

Bravais lattice	Polar anisotropy $\mathcal{A}_j^{(p)}(\omega)$	Azimuthal anisotropy $\mathcal{A}_j^{(a)}(\omega)$
aP (triclinic) mP, mC (monoclinic) oP, oC, oI, oF (orthorhombic)	$\neq 0$	$\neq 0$
tP, tI (tetragonal) hR (trigonal) hP (hexagonal)	$\neq 0$	0
cP, cI, cF (cubic)	0	0

where the polar and azimuthal anisotropy is determined by $\mathcal{A}_j^{(p)}$ and $\mathcal{A}_j^{(a)}$, respectively. Y_{LM} are spherical harmonic functions. In table 1, constraints on the vibrational anisotropies are listed for the Bravais lattices. In general, the local DOS and the anisotropy functions can be determined from data at three properly chosen angle pairs (θ, φ). Systems with one $(n \geqslant 3)$-fold rotation axis show axial symmetry, e.g., crystals with hexagonal unit cell, thin films, and multilayers. Two different angles θ are then sufficient to determine local DOS and the anisotropy function. If several $(n \geqslant 3)$-fold rotation axes exist, $\mathcal{A}_j$ vanishes.

We return now to eq. (58) and cast our result into a more familiar form. The nth term of the series expansion of the exponential represents the n-particle contribution to the self-intermediate scattering function. We obtain

$$L_j(\mathbf{k}, t) = L_{\mathrm{cms}}(k, t)\, F_j(\mathbf{k}) \sum_{n=0}^{\infty} \frac{(f_j(\mathbf{k}, t))^n}{n!}, \tag{62}$$

where $F_j(\mathbf{k}) = \exp(-f_j(\mathbf{k}, 0))$ denotes the local and anisotropic Lamb–Mössbauer factor. The generating function for the n-particle contributions and its Fourier transform are given by

$$\begin{aligned} f_j(\mathbf{k}, t) &= \int \frac{\omega_{\mathrm{R}}}{\omega} g_j(\mathbf{s}, \omega)\big((1 + n_\omega)\, \mathrm{e}^{-\mathrm{i}\omega t} + n_\omega \mathrm{e}^{\mathrm{i}\omega t}\big)\, \mathrm{d}\omega, \\ \tilde{f}_j(\mathbf{k}, \omega) &= 2\pi \frac{\omega_{\mathrm{R}} g_j(\mathbf{s}|\omega|)}{\omega(1 - \exp(-\beta\omega))}. \end{aligned} \tag{63}$$

In the spectrum of L_j, the n-particle contribution emerges as the n-fold convolution of the single-particle term $\tilde{f}_j$ with itself. These expressions are formally identical with results of Singwi and Sjölander [5] for isotropic crystals and Kohn et al. [38] for anisotropic crystals. The function $g_j(\mathbf{s}, \omega)$ is well defined by eqs. (59) and (60) for the discussed model of a thermalized ensemble of harmonically coupled atoms.

If we assume translational symmetry of the lattice one can show with the results of appendix D that eq. (59) takes the form

$$g_p(\mathbf{s},\omega) = \frac{1}{N_0}\sum_{mK} \left|\mathbf{s}\cdot\mathbf{e}_{pm}^{(K)}\right|^2 \delta\left(\omega-\omega_m^{(K)}\right). \tag{64}$$

In this expression the index p enumerates atoms in the symmetry unit, the index m enumerates phonon modes, and the index K is identified with the "quasimomentum" of the phonon. A phonon of mode m and quasimomentum K has energy $\omega_m^{(K)}$ and polarization vector $\mathbf{e}_{pm}^{(K)}$ at atom p in the symmetry unit.

6. Conclusion

In this paper, we studied incoherent NRS in the more general context of X-ray scattering processes in matter. A modern approach of using perturbative solutions of QED leads to a classification of X-ray scattering problems. In the weak field regime, one can clearly distinguish incoherent, coherent elastic, and coherent inelastic scattering processes. The connection between atomic vibrations and X-ray scattering emerges on a basic level. A study of incoherent scattering channels involving NRS on single atoms provided time- and angle-dependent scattering intensities. Also the influence of atomic vibrations materialized in the form of a self-intermediate scattering function, which is well known to comprise single-atom properties in many-atom systems. The study of molecules in gases or liquids and other systems with rotational degrees of freedom requires a more sophisticated approach that would go beyond the scope of this paper. One would replace, e.g., $\hat{j}_\mu(x) \to \widehat{R}_{\mu\nu}(t)\hat{j}_\nu(x)$, where the rotation matrix $\widehat{R}_{\mu\nu}$ depends on the dynamical variables of the atomic motion. The lattice function $\mathcal{L}$ defined in eq. (26), as well as the self-intermediate scattering function L defined by eq. (33), will assume a tensor character, i.e., $\mathcal{L}\mathbf{N}_{\mu\nu} \to \mathcal{L}_{\mu\nu\sigma\lambda}\mathbf{N}_{\sigma\lambda}$ in eq. (25) and $L\,N \to L_{\mu\nu}\,N_{\mu\nu}$ in eqs. (31), (40). The factorization of lattice and nuclear properties becomes difficult and the interpretation more complicated. The treatment of macroscopic samples containing large numbers of atoms requires consideration of all important X-ray scattering channels, which may cause a serious complication. However, incoherent NRS dominates the resonant scattering channels even for large samples, unless incident X-rays directly excite the nuclear resonance. This finding is so far supported by experiments [11,12,14]. At present it seems quite clear that incoherent NRS provides direct and local access to the self-intermediate scattering function. The extreme selectivity to the nuclear resonant isotope is unique and unheard of in other X-ray scattering techniques or in neutron scattering methods. Two examples, the ideal gas and the harmonic lattice, were selected to demonstrate methods of calculating the self-intermediate scattering function. The results from the harmonic lattice model extend previous treatments of single crystals to disordered and amorphous systems. In isotropic systems, the self-intermediate scattering function is completely constructed from the local vibrational DOS. Anisotropic systems require two additional energy-dependent functions

for a complete description. The relationship between self-intermediate scattering function and vibrational DOS plus anisotropy terms is invertible, and the harmonic lattice provides an attractive model for data evaluation.

Acknowledgements

WS is grateful to E.E. Alp, T.S. Toellner, and A.I. Chumakov for fruitful discussions. This work was supported by the U.S. Department of Energy, Basic Energy Sciences, Office of Science, under Contract No. W-31-109-Eng-38.

Appendix A

The evaluation of the scattering matrix defined by eq. (9) has been discussed extensively in the past. The perturbation expansion of the operator $\widehat{S}$ defined by eq. (5) in combination with time ordering produces a multitude of individual terms. From a physical standpoint this is plausible because the eigenstates of the charge distribution are not simply given by the eigenstates of the non-interacting system. They rather develop slowly from the distant past when the interaction is "switched on" according to eq. (2). An excellent description of nuclear resonant scattering is obtained in the "ladder approximation". In the center of mass system of the atom, the scattering matrix takes the form

$$\mathbf{M}_{fi}(x,x') = -\mathrm{i}\lim_{t_0\to\infty}\langle\phi_f|\,\widehat{G}(t_0-t)\,\hat{\mathbf{j}}(\mathbf{x})\widehat{G}(t-t')\hat{\mathbf{j}}(\mathbf{x}')\widehat{G}(t'-t_0)\,|\phi_i\rangle. \qquad \text{(A.1)}$$

$\widehat{G}$ assumes the role of a future directed time development operator of the eigenstates of the interacting system. The structure of $\widehat{G}$ is illustrated in figure 4, where the "blobs" symbolize the interaction that perturbs the non-interacting time development operator. $\widehat{G}$ is also the solution of Dyson's equation

$$\begin{aligned}\widehat{G}(t-t') &= \widehat{G}_0(t-t') + \int \widehat{G}_0(t-\tau)\widehat{V}(\tau-\tau')\widehat{G}_0(\tau'-t')\,\mathrm{d}\tau\,\mathrm{d}\tau' \\ &\quad + \int \widehat{G}_0(t-\tau)\widehat{V}(\tau-\tau')\widehat{G}_0(\tau'-\tau'')\widehat{V}(\tau'-\tau'') \\ &\quad \times \widehat{G}_0(\tau''-t')\,\mathrm{d}\tau\,\mathrm{d}\tau'\,\mathrm{d}\tau'' + \cdots \\ &= \widehat{G}_0(t-t') + \int \widehat{G}_0(t-\tau)\widehat{V}(\tau-\tau')\widehat{G}(\tau'-t')\,\mathrm{d}\tau\,\mathrm{d}\tau'. \qquad \text{(A.2)}\end{aligned}$$

The perturbation and thus the effects of the electromagnetic self-action are contained in the operator $\widehat{V}$. The future directed time development operator of the non-interacting system is obtained from eqs. (2) and (16):

$$\widehat{G}_0(t) = \Theta(t)\mathrm{e}^{-\mathrm{i}\widehat{H}_N t} = \mathrm{i}\lim_{\varepsilon\to+0}\int \frac{\mathrm{e}^{-\mathrm{i}\omega t}}{\omega-\widehat{H}_N+\mathrm{i}\varepsilon}\frac{\mathrm{d}\omega}{2\pi}. \qquad \text{(A.3)}$$

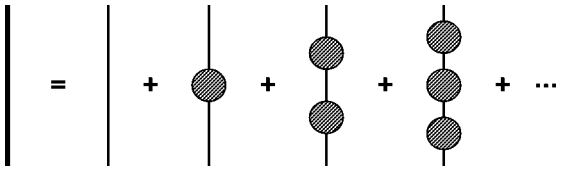

Figure 4. Graphical representation of eq. (A.2) showing the propagator of the interacting nucleus. The thin lines stand for the propagator of the non-interacting nucleus given by eq. (A.3). The perturbation $\widehat{V}$ acting on the nucleus is illustrated by the blobs.

Introducing the Fourier image $\widehat{\Delta}$ of the perturbation operator, eq. (A.2) is solved by

$$\widehat{G}(t) = \mathrm{i} \int \frac{\mathrm{e}^{-\mathrm{i}\omega t}}{\omega - \widehat{H}_N - \mathrm{i}\widehat{\Delta}(\omega)} \frac{\mathrm{d}\omega}{2\pi}. \tag{A.4}$$

This expression is just eq. (A.3) with the replacement $\widehat{H}_N \rightarrow \widehat{H}_N + \mathrm{i}\widehat{\Delta}$, where $\widehat{\Delta}$ is known as the level shift operator. A diagonal representation of the propagator $\widehat{G}$ would require one to find the eigenvalues and eigenstates of the operator $\widehat{H}_N + \mathrm{i}\widehat{\Delta}$. However, the perturbations can be assumed small, and $\widehat{\Delta}$ is almost diagonal in the eigenstates of $\widehat{H}_N$. The approximate matrix elements are then

$$\langle \phi_n | \big(\widehat{H}_N + \mathrm{i}\widehat{\Delta}\big) | \phi_{n'} \rangle = \left(\omega_n + \varepsilon_n - \mathrm{i}\frac{\Gamma_n}{2}\right)\delta_{nn'}, \tag{A.5}$$

where ω_n is the eigenvalue of $\widehat{H}_N$ corresponding to eigenstate $|\phi_n\rangle$, $\varepsilon_n = -\Im\langle\phi_n| \times \widehat{\Delta}|\phi_n\rangle$ gives the shift of the energy level caused by the interaction with the photon field, and $\Gamma_n = -2\Re\langle\phi_n|\widehat{\Delta}|\phi_n\rangle$ describes the line broadening of the state $|\phi_n\rangle$. With these abbreviations, eq. (A.4) assumes the form

$$\widehat{G}(t) = \mathrm{i} \sum_n |\phi_n\rangle \int \frac{\mathrm{e}^{-\mathrm{i}\omega t}}{\omega - \omega_n - \varepsilon_n(\omega) + \mathrm{i}\frac{1}{2}\Gamma_n(\omega)} \frac{\mathrm{d}\omega}{2\pi} \langle\phi_n|. \tag{A.6}$$

Further evaluation is complicated by the fact that level shift, as well as line width, appears to be a function of energy. This functional dependence on energy, however, is weak, and we may replace ω with ω_n in the arguments. The integration is then straightforward, and one obtains

$$\widehat{G}(t) = \Theta(t) \sum_n |\phi_n\rangle \mathrm{e}^{-(\mathrm{i}\omega_n + \mathrm{i}\varepsilon_n + (\Gamma_n/2))t} \langle\phi_n|, \tag{A.7}$$

where ε_n and $\Gamma_n > 0$ are evaluated at $\omega = \omega_n$. Before we complete our derivation of the scattering matrix, we will briefly discuss the construction of the operator $\widehat{V}$. Figure 5 displays a perturbation expansion of $\widehat{V}$ in terms of compact Feynman diagrams.

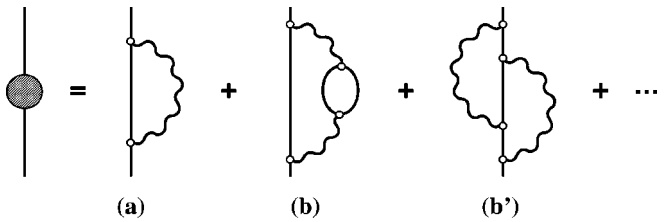

Figure 5. Feynman diagrams representing the perturbation expansion of the level shift operator. Panel (a) gives the radiative contribution, which is the only term with only two vertices. Diagrams (b) and (b') are of fourth order. Whereas panel (b), which involves electronic currents symbolized by the closed loop, contributes the considerable internal conversion part to the nuclear level width, the higher order radiative term in panel (b') is negligible.

The lowest order contribution, which is shown in panel (a), is known as the radiative term and can be expressed as

$$\widehat{V}(t) = -\mathrm{i}\int \hat{j}_\mu(\mathbf{x})\delta_+\big(\mathbf{x}-\mathbf{x}',t\big)\widehat{G}_0(t)\hat{j}_\mu\big(\mathbf{x}'\big)\,\mathrm{d}^3x\,\mathrm{d}^3x', \tag{A.8}$$

where the photon propagator is taken from eq. (8) and $\hat{j}_\mu(\mathbf{x})$ are nuclear current operators at $t = 0$. From the previous equation we obtain after some manipulations

$$\begin{aligned}\varepsilon_n &= \frac{1}{\pi}\sum_l \int \frac{j_\mu^{nl}(\mathbf{x})j_\mu^{ln}(\mathbf{x}')}{|\mathbf{x}-\mathbf{x}'|}\int_0^\infty \frac{\sin k|\mathbf{x}-\mathbf{x}'|}{k-\omega_{nl}}\,\mathrm{d}k\,\mathrm{d}^3x\,\mathrm{d}^3x',\\ \Gamma_n &= -2\sum_l \Theta(\omega_{nl})\int j_\mu^{nl}(\mathbf{x})\frac{\sin\omega_{nl}|\mathbf{x}-\mathbf{x}'|}{|\mathbf{x}-\mathbf{x}'|}j_\mu^{ln}\big(\mathbf{x}'\big)\,\mathrm{d}^3x\,\mathrm{d}^3x',\end{aligned} \tag{A.9}$$

where the j_μ^{ln} are matrix elements of the nuclear current operators and ω_{nl} is the energy difference of states $|\phi_n\rangle$ and $|\phi_l\rangle$. For the ground state, the line width Γ_n vanishes as expected because $\omega_{nl} \leqslant 0$. Equation (A.9) describes the radiative contribution as illustrated by figure 5(a). In similar fashion, one obtains the internal conversion term, which is represented by panel (b) of figure 5. ε_n and Γ_n can thus be understood as the total line shift and level broadening, respectively. Keeping this is mind, we insert eq. (A.7) into eq. (A.1):

$$\mathsf{M}_{fi}\big(x,x'\big) = -\mathrm{i}\Theta\big(t-t'\big)\mathrm{e}^{-\mathrm{i}\omega'_{fi}t}\sum_n \mathrm{e}^{-(\mathrm{i}\omega_{ni}+\mathrm{i}\varepsilon_{ni}+\Gamma_n/2)(t-t')}\mathbf{j}^{fn}(\mathbf{x})\mathbf{j}^{ni}\big(\mathbf{x}'\big), \tag{A.10}$$

where ω'_{fi} denotes the energy transfer to the nucleus. Usually the low-energy nuclear states are well separated in energy and degenerate if hyperfine interactions vanish. To emphasize this situation we rewrite eq. (A.10) for the ground state $|\phi_{Gi}\rangle$ and one group of excited states $|\phi_{Nn}\rangle$, where n, i describe degeneracy:

$$\begin{aligned}\mathsf{M}_{fi}\big(x,x'\big) = -\mathrm{i}\Theta\big(t-t'\big)\mathrm{e}^{-\mathrm{i}\omega'_{fi}t}\mathrm{e}^{-(\mathrm{i}\omega_N+\Gamma/2)(t-t')}\\ \times\sum_n\langle\phi_{Gf}|\hat{\mathbf{j}}(\mathbf{x})|\phi_{Nn}\rangle\langle\phi_{Nn}|\hat{\mathbf{j}}\big(\mathbf{x}'\big)|\phi_{Gi}\rangle.\end{aligned} \tag{A.11}$$

ω_N and Γ have the natural meaning of nuclear transition energy and nuclear line width associated with a particular group of degenerate excited states. Equation (A.11) easily extends to cases with static hyperfine interactions being present. Let $\widehat{H}_{\rm hf}$ be the Hamiltonian of the hyperfine interactions and $\widehat{U}_{\rm hf}(t) = \exp(-{\rm i}\widehat{H}_{\rm hf}t)$. Then one obtains

$$\mathbf{M}_{fi}(x,x') = -{\rm i}\Theta(t-t'){\rm e}^{-{\rm i}\omega'_{fi}t}{\rm e}^{-({\rm i}\omega_N+\Gamma/2)(t-t')} \times \sum_n \langle\phi_{Gf}|\,\hat{\mathbf{j}}(\mathbf{x})|\phi_{Nn}\rangle\langle\phi_{Nn}|\widehat{U}_{\rm hf}(t-t')\hat{\mathbf{j}}(\mathbf{x}')\widehat{U}^\dagger_{\rm hf}(t-t')|\phi_{Gi}\rangle, \quad \text{(A.12)}$$

where ω_N and Γ retain their previously given meanings because their change brought about by the hyperfine interactions is negligible.

Appendix B

In this section, the normalization of the time-dependent angular correlation functions for nuclear resonant fluorescence, eq. (32), and internal conversion followed by atomic fluorescence, eq. (41), will be discussed. We will make the reasonable assumption that the nuclear ground and excited state have spin quantum numbers I, I' and the degeneracy is described by magnetic quantum numbers m, m'. The transition currents in the expression for the radiative contribution to the line width, eq. (A.9), are then replaced by their Fourier transforms to give

$$\frac{\Gamma}{1+\alpha} = -\frac{\omega_N}{2\pi}\sum_m \int \big\langle I'm'\big|\hat{J}_\mu(-\mathbf{k})|Im\rangle\langle Im|\hat{J}_\mu(\mathbf{k})\big|I'm'\big\rangle\,{\rm d}\Omega_k. \quad \text{(B.1)}$$

The integration is over all directions of $\mathbf{k}$ and $|\mathbf{k}| = \omega_N$. Although all the components of the current four-vector appear in eq. (B.1), we can use the continuity equation to infer $\omega_N\, J_0(\mathbf{k}) = \mathbf{k}\cdot\mathbf{J}(\mathbf{k})$ for the quasimonochromatic transition currents. This relationship, inserted into eq. (B.1), only leaves us with the transverse transition currents

$$\frac{\Gamma}{1+\alpha} = \frac{\omega_N}{2\pi}\sum_m \int \big\langle I'm'\big|\widehat{\mathbf{J}}(-\mathbf{k})|Im\rangle\langle Im|\widehat{\mathbf{J}}(\mathbf{k})\big|I'm'\big\rangle\,{\rm d}\Omega_k. \quad \text{(B.2)}$$

If we assume that the nuclear current operators only facilitate transitions between the degenerate states $|I\rangle$ and $|I'\rangle$, we obtain the following compact form:

$$\int \langle\phi_n|\,\widehat{\mathbf{J}}^\dagger(-\mathbf{k}_S)\widehat{\mathbf{J}}(-\mathbf{k}_S)|\phi_{n'}\rangle\,{\rm d}\Omega = \frac{2\pi\Gamma}{k_S(1+\alpha)}\delta_{nn'}. \quad \text{(B.3)}$$

Equation (B.2) is also used for the normalization of the multipole expansion of the nuclear transition currents [23]. We may write for the matrix element of the transverse nuclear current operator

$$\big\langle I'm'\big|\widehat{\mathbf{J}}(\mathbf{k})|Im\rangle = \sqrt{\frac{2\pi\Gamma}{k(1+\alpha)}}\sum_{\rm LM\lambda}\varepsilon_{L\lambda}C\big(I\,L\,I';m\,M\,m'\big)\mathbf{Y}^{(\lambda)\,*}_{\rm LM}\left(\frac{\mathbf{k}}{k}\right). \quad \text{(B.4)}$$

The $\mathbf{Y}^{(\lambda)}_{\mathrm{LM}}$ is a transverse vector spherical harmonic describing magnetic ($\lambda = 0$) or electric ($\lambda = 1$) multipole radiation of order L. The multipole mixing coefficients $\varepsilon_{L\lambda}$ are normalized, $\sum_{L\lambda} |\varepsilon_{L\lambda}|^2 = 1$. $C(\ldots)$ are Clebsch–Gordan coefficients in the notation of Rose [42]. The previous equations permit us to write

$$\int \left\langle \sum_f \left| \mathbf{N}_{fi}(-\mathbf{k}_S, \mathbf{k}_0, t)\, \mathbf{p} \right|^2 \right\rangle \mathrm{d}\Omega = \frac{2\pi\Gamma}{k_S(1+\alpha)} \left\langle \mathbf{p}^* \cdot \hat{\mathbf{J}}^\dagger(\mathbf{k}_0) \mathbf{p} \cdot \hat{\mathbf{J}}(\mathbf{k}_0) \right\rangle$$
$$= \frac{\pi\Gamma^2}{2\omega_N^2(1+\alpha)^2} \frac{2I'+1}{2I+1} = \frac{\sigma\Gamma^2}{4(1+\alpha)}. \quad \text{(B.5)}$$

The second line was obtained under the assumptions that $k_0 \approx k_S \approx \omega_N$ and that the ensemble of nuclei is unpolarized, i.e., the occupation numbers for the possible nuclear ground states are equal. σ is the nuclear resonant cross section. Substitution of the previous equation into the integrated eq. (32) gives

$$\int N(\mathbf{k}_S, \mathbf{k}_0, t)\, \mathrm{d}\Omega = 1 - \frac{4(1+\alpha)}{\sigma\Gamma^2} \frac{1}{2I+1} \sum_i \int \left| \mathbf{N}_{ii}(-\mathbf{k}_S, \mathbf{k}_0, t) \mathbf{p} \right|^2 \mathrm{d}\Omega. \quad \text{(B.6)}$$

There is no simple expression for the second term of the right-hand side of the equation. In general, it will show a complicated behavior in time and as a function of direction and polarization of the incident radiation. However, the term will always be positive and less than unity and can be estimated by averging over direction and polarization of the incident radiation. If we assume that the magnetic quantum numbers are good quantum numbers to describe the nuclear states, we obtain

$$\overline{\frac{1}{4\pi} \int N(\mathbf{k}_S \mathbf{k}_0, t)\, \mathrm{d}\Omega\, \mathrm{d}\Omega_0}$$
$$= 1 - \frac{1}{2I'+1} \sum_{ni} \left(\sum_{L\lambda} |\varepsilon_{L\lambda}|^2 C^2\big(ILI'; m_i\, m_n - m_i\big) \right)^2. \quad \text{(B.7)}$$

For resonant isotopes with pure dipole transitions $L = 1$ and nuclear spin quantum numbers $I = 1/2$ and $I' = 3/2$, one obtains $29/36$ for the averaged angular correlation function.

We now turn our attention to the angular correlation function describing internal conversion followed by atomic fluorescence, eq. (41). It will be convenient to write the quantum states of the scatterer as the product of nuclear states $|\psi\rangle$ and electronic states $|\beta\rangle$, e.g., $|\phi_i\rangle = |\beta_i\rangle|\psi_i\rangle$. We also need a more general formulation of eq. (B.3) for the case of electronic currents because the intermediate electronic states may be superpositions of total angular momentum states $|S\, l\rangle$, e.g., $|\beta_n\rangle = \sum_{Sl} |S\, l\rangle\langle S\, l|\beta_n\rangle$. First we use a multipole expansion of the current operators and apply the Wigner–Eckart theorem to each term. The execution of the sum over final electronic states and averaging over initial electronic states is problematic because the energy of the fluorescence radiation depends on initial and final states via $k_S = k_0 - \omega_{fi}$. But we

can assume that the dependence of ω_{fi} on magnetic quantum numbers is negligible. Under these circumstances one obtains after some manipulations

$$\int \langle Sl|\widehat{\mathbf{S}}^{\dagger}(-\mathbf{k}_S)\widehat{\mathbf{S}}(-\mathbf{k}_S)\big|S'\,l'\big\rangle \,\mathrm{d}\Omega = \delta_{ll'}\delta_{SS'}a_{Si}, \tag{B.8}$$

where a_{Si} depends on quantum numbers of the intermediate and initial electronic state. We may now write

$$\begin{aligned}\int \Big\langle \sum_f \big|\mathbf{N}'_{fi}(-\mathbf{k}_S,\mathbf{k}_0,t)\mathbf{p}\big|^2 \Big\rangle \,\mathrm{d}\Omega \\ = \sum_{S'l'mi} w_i \big|\langle S\,l|\langle I\,m|\widehat{B}\,\widehat{U}_N^{\dagger}(t)\mathbf{p}\cdot\hat{\mathbf{J}}(\mathbf{k}_0)|\psi_i\rangle|\beta_i\rangle\big|^2,\end{aligned} \tag{B.9}$$

where w_i is the weight of the initial state $|\psi_i\rangle|\beta_i\rangle$. The same method that we used to obtain eq. (B.8) is applied to calculate the matrix elements of the operator $\widehat{B}$ as given by eq. (39). In particular, one obtains

$$\begin{aligned}\sum_{mll'} \langle S\,l|\big\langle I'\,m'\big|\widehat{B}^{\dagger}|I\,m\rangle\big|S'\,l'\big\rangle\big\langle S'\,l'\big|\langle Im|\widehat{B}\big|I'\,m''\big\rangle|S\,l\rangle \\ = \delta_{m'm''}B_{SS'}\frac{2\pi\Gamma}{\omega_N(1+\alpha)},\end{aligned} \tag{B.10}$$

where $B_{SS'}$ is a sum composed of reduced electronic matrix elements and the multipole mixing coefficients of the nuclear transition. $B_{SS'}$ also contains a resonant denominator selecting initial electronic states $|S\,l\rangle$ and intermediate electronic states $|S'\,l'\rangle$ for which the energy difference matches the nuclear transition energy ω_N within the line width of the intermediate electronic state. Finally, we arrive at

$$\int \Big\langle \sum_f \big|\mathbf{N}'_{fi}(-\mathbf{k}_S,\mathbf{k}_0,t)\mathbf{p}\big|^2 \Big\rangle \,\mathrm{d}\Omega = \frac{\sigma\Gamma^2}{4(1+\alpha)}\sum_{SS'} w_S\, B_{SS'}\, a_{S'}. \tag{B.11}$$

An interpretation of the sum on the right-hand side of the equation is obtained from the well-known ratio of the integrated scattering probabilities for a single atom:

$$\frac{\int\langle\sum_f |\mathbf{N}'_{fi}(-\mathbf{k}_S,\mathbf{k}_0,t)\,\mathbf{p}|^2\rangle\,\mathrm{d}\Omega}{\int\langle\sum_f |\mathbf{N}_{fi}(-\mathbf{k}_S,\mathbf{k}_0,t)\mathbf{p}|^2\rangle\,\mathrm{d}\Omega} = \sum_{SS'} w_S\, B_{SS'}\, a_{S'} = \sum_n \alpha_n\eta_n. \tag{B.12}$$

α_n is the partial internal conversion coefficient of the nuclear transition and $\sum_n \alpha_n = \alpha$. The fluorescence yield η_n gives the probability for the emission of a fluorescence photon following the particular internal conversion process. The index n usually refers to K, L, etc., conversion.

Appendix C

It is sufficient to calculate the scattering matrix that corresponds to diagram (c) in figure 2 in the center of mass system of the nucleus. The main contributions come from resonant scattering processes involving the nuclear resonance and an electronic resonance, e.g., the creation of a core hole. Whereas the influence of the electrons has to be considered for the calculation of the nuclear level width, the electronic resonances can be treated independently of nuclear properties other than total charge. An excellent approximation for the scattering matrix is obtained if the nuclear scattering contribution is taken from eq. (25) and extended by the resonant electronic part:

$$\begin{aligned}\mathbf{M}_{fi}(x,x') = -\mathrm{i}\int \langle\phi_f|\hat{\mathbf{s}}(x)\Theta(t-t_y)\,\mathrm{e}^{-\hat{\Delta}(t-t_y)}\hat{s}_\mu(y)\delta_+(y-y')\hat{j}_\mu(y') \\ \times\,\Theta(t_{y'}-t')\mathrm{e}^{-(\Gamma/2)(t_{y'}-t')}\hat{\mathbf{j}}(x')|\phi_i\rangle\,\mathrm{d}y\,\mathrm{d}y', \qquad \text{(C.1)}\end{aligned}$$

where $\widehat{\Delta}$ is the electronic level shift operator. One of the time integrations can be eliminated by using $\delta_+(y) = \delta(|t|-|\mathbf{y}|)/|\mathbf{y}|$. Also the time dependence of the nuclear current that couples to the electronic current can be approximated by a simple phase factor $\exp(\mathrm{i}\omega_N t)$. After some manipulations we obtain for the integral

$$\begin{aligned}\mathrm{e}^{-(\Gamma/2)(t-t')}\int \Theta(\tau)\mathrm{e}^{-(\hat{\Delta}-\Gamma/2-\mathrm{i}\omega_N)\tau}\frac{\hat{s}_\mu(\mathbf{y},t-\tau)\hat{j}_\mu(\mathbf{y}',t)}{|\mathbf{y}-\mathbf{y}'|} \\ \times\left\{\Theta\big(t-t'-\tau-|\mathbf{y}-\mathbf{y}'|\big)\mathrm{e}^{(\Gamma/2+\mathrm{i}\omega_N)|\mathbf{y}-\mathbf{y}'|}\right. \\ \left.+\,\Theta\big(t-t'-\tau+|\mathbf{y}-\mathbf{y}'|\big)\mathrm{e}^{-(\Gamma/2+\mathrm{i}\omega_N)|\mathbf{y}-\mathbf{y}'|}\right\}\mathrm{d}^3y\,\mathrm{d}^3y'\,\mathrm{d}\tau. \qquad \text{(C.2)}\end{aligned}$$

The major contribution to the volume integrals comes from regions of high nuclear and core electron current density, where the distance $|\mathbf{y}-\mathbf{y}'|$ is of the order of the atomic size. For all electronic resonances, we have $\Gamma \ll \Delta_n \ll 1/|\mathbf{y}-\mathbf{y}'|$ and several related terms can be neglected, providing the result

$$\begin{aligned}\Theta(t-t')\mathrm{e}^{-(\Gamma/2)(t-t')}\int_0^{t-t'}\mathrm{d}\tau\mathrm{e}^{-(\hat{\Delta}-\mathrm{i}\omega_N)\tau} \\ \times\int \hat{s}_\mu(\mathbf{y},t-\tau)\frac{\cos\omega_N|\mathbf{y}-\mathbf{y}'|}{|\mathbf{y}-\mathbf{y}'|}\hat{j}_\mu(\mathbf{y}',t)\mathrm{d}^3y\,\mathrm{d}^3y'. \qquad \text{(C.3)}\end{aligned}$$

The upper limit of the time integral can safely be extended to infinity. This approximation affects only behavior at very early times $\Delta_n(t-t') \approx 1$, which is not relevant in this context. Using relations of the type $\hat{s}_\mu(t) = \widehat{U}_N^\dagger(t)\hat{s}_\mu(0)\widehat{U}_N(t)$ and substituting the previous result into the integral in eq. (C.1), we arrive at

$$\begin{aligned}\mathbf{M}_{fi}(x,x') = -\mathrm{i}\Theta(t-t')\mathrm{e}^{-(\Gamma/2)(t-t')}\mathrm{e}^{\mathrm{i}\omega_{fi}t} \\ \times\,\langle\phi_f|\hat{\mathbf{s}}(\mathbf{x})\widehat{B}\widehat{U}_N(t-t')\hat{\mathbf{j}}(\mathbf{x}')\widehat{U}_N^\dagger(t-t')|\phi_i\rangle, \qquad \text{(C.4)}\end{aligned}$$

where $\widehat{B}$ is given by eq. (39). The effect of lattice vibrations can be included by replacing $\hat{\mathbf{s}}$ and $\hat{\mathbf{j}}$ according to $\hat{\mathbf{s}}(\mathbf{x}) \rightarrow \hat{\mathbf{s}}(\mathbf{x}+\hat{\mathbf{r}}(t))$ with the atomic displacement operator $\hat{\mathbf{r}}$. Using spatial Fourier transforms of $\hat{\mathbf{s}}$ and $\hat{\mathbf{j}}$ directly leads to

$$\begin{aligned}\mathbf{M}_{fi}\big(x,x'\big) = -\mathrm{i}\Theta\big(t-t'\big)\mathrm{e}^{\mathrm{i}\omega_{fi}t}\mathrm{e}^{-(\mathrm{i}\omega_N+\Gamma/2)(t-t')} \\ \times \int \mathcal{L}_{fi}\big(\mathbf{k},\mathbf{k}',t-t'\big)\mathbf{N}'_{fi}\big(\mathbf{k},\mathbf{k}',t-t'\big)\mathrm{e}^{\mathrm{i}(\mathbf{k}\cdot\mathbf{x}+\mathbf{k}'\cdot\mathbf{x}')}\frac{\mathrm{d}^3k\,\mathrm{d}^3k'}{(2\pi)^6},\end{aligned} \quad \text{(C.5)}$$

where ω_{fi} includes the energy transfer to lattice, nucleus, and electron shell. $\mathcal{L}_{fi}$ and $\mathbf{N}'_{fi}$ are defined by eqs. (26) and (38).

Appendix D

We start with the Hamiltonian of the harmonic lattice in the center of mass system given by

$$\widehat{H} = \sum_j \frac{\hat{\mathbf{p}}_j^2}{2\,m_j} + \frac{1}{2}\sum_{jj'} \hat{\mathbf{u}}_j \mathbf{D}_{jj'} \hat{\mathbf{u}}_{j'}, \quad \text{(D.1)}$$

where the sums run over all but one atom of the ensemble, i.e., the force constant matrix is nonsingular. In the following treatment, we will use the indices l, l' to enumerate degrees of freedom or particle modes and indices j, j' to enumerate atoms of the ensemble. The dynamical variables corresponding to the translational degrees of freedom are displacements and momenta $\{\hat{u}_l, \hat{p}_l\}$, which follow the usual commutation relations, i.e., $[\hat{u}_l, \hat{p}_{l'}] = \mathrm{i}\,\delta_{ll'}$. In the Heisenberg picture, the dynamical equations for the operators are

$$\hat{\mathbf{p}}_j = m_j \frac{\mathrm{d}\hat{\mathbf{u}}_j}{\mathrm{d}t}, \qquad m_j \frac{\mathrm{d}^2\hat{\mathbf{u}}_l}{\mathrm{d}t^2} = -\sum_{j'} \mathbf{D}_{jj'}\hat{\mathbf{u}}_{j'}. \quad \text{(D.2)}$$

This set of equations is simplified by introducing a new set of operators $\{\hat{a}_l, \hat{a}_l^\dagger\}$ obtained from $\{\hat{u}_l, \hat{p}_l\}$ by a linear transformation. Let $\mathbf{X}_{jl}$ be the unitary matrix that diagonalizes the matrix $\mathbf{D}_{jj'}/\sqrt{m_j\,m_{j'}}$ with eigenvalues $\omega_l^2 > 0$:

$$\sum_{jj'} \mathbf{X}_{lj}^\dagger \frac{\mathbf{D}_{jj'}}{\sqrt{m_j\,m_{j'}}} \mathbf{X}_{j'l'} = \omega_l^2\,\delta_{ll'}. \quad \text{(D.3)}$$

Then the replacements ($\omega_l > 0$)

$$\begin{aligned}\hat{\mathbf{u}}_j &= \frac{1}{\sqrt{2m_j}}\sum_l \frac{1}{\sqrt{\omega_l}}\big(\mathbf{X}_{jl}^*\hat{a}_l^\dagger + \mathbf{X}_{jl}\hat{a}_l\big), \\ \hat{\mathbf{p}}_j &= \mathrm{i}\sqrt{\frac{m_j}{2}}\sum_l \sqrt{\omega_l}\big(\mathbf{X}_{jl}^*\hat{a}_l^\dagger - \mathbf{X}_{jl}\hat{a}_l\big)\end{aligned} \quad \text{(D.4)}$$

result in decoupled dynamical equations and simple nonvanishing commutators of the form

$$\frac{\mathrm{d}\hat{a}_l}{\mathrm{d}t} = -\mathrm{i}\omega_l \hat{a}_l, \qquad \frac{\mathrm{d}\hat{a}_l^\dagger}{\mathrm{d}t} = \mathrm{i}\omega_l \hat{a}_l^\dagger, \qquad [\hat{a}_l, \hat{a}_{l'}^\dagger] = \delta_{ll'}. \tag{D.5}$$

$\hat{a}_l^\dagger$ and $\hat{a}_l$ are known as creation and annihilation operators of a particle in mode l, and they provide a bosonic particle interpretation of the harmonic lattice excitations. Stable systems have to satisfy $\forall_l$ ($\omega_l^2 > 0$). Solving the eigenvalue problem posed by eq. (D.3) for a given macroscopic ensemble is a formidable task. One usually introduces translational symmetries to reduce the workload, and very good descriptions of vibrations in single crystals or polycrystalline materials can be obtained [10]. Disordered or amorphous materials were also modeled using harmonic interactions [39,40].

In the particle representation, the Hamiltonian takes the simple form

$$\widehat{H} = \sum_l \widehat{H}_l = \sum_l \omega_l \left(\hat{a}_l^\dagger \hat{a}_l + \frac{1}{2} \right). \tag{D.6}$$

The particle modes are decoupled, i.e., $[\widehat{H}_l, \widehat{H}_{l'}] = 0$, and therefore the eigenstates $|\{n_l\}\rangle$ of the Hamiltonian are easily constructed as a product of eigenstates for the individual modes

$$\big|\{n_l\}\big\rangle = \prod_l \frac{(\hat{a}_l^\dagger)^{n_l}}{\sqrt{n_l!}} |0\rangle. \tag{D.7}$$

Here n_l is the number of particles in mode l, and $|0\rangle$ is the ground state. We also find that the self-intermediate scattering function factorizes, and the individual factors are given by

$$L_{jl}(\mathbf{k}, t) = \frac{\mathrm{Trace}\{\mathrm{e}^{-\beta\widehat{H}_l} \widehat{T}_l(\alpha_{jl}\mathrm{e}^{\mathrm{i}\omega_l t}) \widehat{T}_l(-\alpha_{jl})\}}{\mathrm{Trace}\{\mathrm{e}^{-\beta\widehat{H}_l}\}}, \quad \alpha_{jl} = \frac{\mathrm{i}\mathbf{k} \cdot \mathbf{X}_{jl}^*}{\sqrt{2m_j\omega_l}}. \tag{D.8}$$

The use of the "translation operator" $\widehat{T}_l(\alpha) = \exp\{\alpha\hat{a}_l^\dagger - \alpha^*\hat{a}_l\}$ is convenient because it generates coherent particle states [41], which form an alternative basis to the particle number states of eq. (D.7). The relationship of a coherent state $|\alpha_l\rangle$ to the number states is

$$|\alpha_l\rangle = \widehat{T}_l(\alpha)|0\rangle, \qquad \widehat{T}_l(\alpha)\widehat{T}_l(\gamma) = \mathrm{e}^{(1/2)(\alpha\gamma^* - \gamma\alpha^*)} \widehat{T}_l(\alpha + \gamma). \tag{D.9}$$

The evaluation of the trace in eq. (D.8) can be conveniently performed using coherent states, and after some manipulations we obtain eq. (57).

In the presence of translational symmetries, the diagonalization in eq. (D.3) can be simplified. Let N be a set of translations that leaves the ensemble unchanged, i.e., $\mathbf{D}_{j+N,j'+N'} = \mathbf{D}_{j,j'+N'-N}$ and $m_{j+N} = m_j$. Then we can write

$$\mathbf{\Omega}_{jj'} = \mathbf{\Omega}_{pp',NN'} = \sum_L \mathbf{\Omega}_{pp',0L} W_{NN'}^{(L)}, \quad W_{NN'}^{(L)} = \frac{1}{2}(\delta_{L,N-N'} + \delta_{L,N'-N}), \tag{D.10}$$

where $\mathbf{\Omega}_{jj'} = \mathbf{D}_{jj'}/\sqrt{m_j m_{j'}}$ and the enumeration of atoms was replaced by a separate enumeration of symmetry units (indices N, N', L) and of atoms within a symmetry unit (indices p, p'). The matrices $W^{(L)}$ commute with each other and can be diagonalized by the same unitary transformation. The eigenvalue problem and its solution are given by

$$\sum_{NN'} \psi^{\dagger}_{KN} W^{(L)}_{NN'} \psi_{N'K'} = \cos(\gamma LK)\delta_{KK'}, \qquad \psi_{NK} = \frac{1}{\sqrt{N_0}}\, \mathrm{e}^{\mathrm{i}\gamma NK}, \tag{D.11}$$

where N_0 is the total number of symmetry units and $\gamma = 2\pi/N_0$. The eigenvector matrix ψ_{NK} is unitary. Equation (D.10) now takes the form

$$\mathbf{\Omega}_{pp',NN'} = \sum_{KK'} \psi_{NK}\, \mathbf{d}^{(K)}_{pp'} \delta_{KK'}\, \psi^{\dagger}_{K'N'}, \quad \mathbf{d}^{(K)}_{pp'} = \sum_{L} \mathbf{\Omega}_{pp',0L} \cos(\gamma LK). \tag{D.12}$$

$\mathbf{d}^{(K)}_{pp'}$ is called the dynamical matrix. The original problem of having to diagonalize one matrix of rank equal to the total number of degrees of freedom has now been reduced to N_0 diagonalizations of the dynamical matrix of the type

$$\sum_{pp'} \mathbf{e}^{(K)\dagger}_{mp} \mathbf{d}^{(K)}_{pp'} \mathbf{e}^{(K)}_{p'm'} = \delta_{mm'}\, \lambda^{(K)}_{m}. \tag{D.13}$$

This equation in combination with eq. (D.10) provides the following relations:

$$\omega^2_l = \lambda^{(K)}_m, \qquad \mathbf{X}_{jl} = \frac{1}{\sqrt{N_0}} \mathbf{e}^{(K)}_{pm} \exp(\mathrm{i}\gamma NK). \tag{D.14}$$

The eigenvectors are periodic, nonlocalized functions on the lattice, and the associated particles are called phonons. In the usual nomenclature, the index p enumerates atoms in the symmetry unit, the index m enumerates phonon modes, and the index K is identified with the "quasimomentum" of the phonon.

References

[1] R.L. Mössbauer, Z. Physik 151 (1958) 124.
[2] Y. Kagan, this issue, section III-1.1, and references therein.
[3] J.P. Hannon and G.T. Trammell, this issue, section III-1.2, and references therein.
[4] W.M. Visscher, Ann. Phys. 9 (1960) 194.
[5] K.S. Singwi and A. Sjölander, Phys. Rev. 120 (1960) 1093.
[6] Y. Kagan and Y.A. Iosilevskii, Zh. Èksper. Teoret. Fiz. 42 (1962) 259, Zh. Èksper. Teoret. Fiz. 44 (1963) 284.
[7] S.L. Ruby, J. Phys. 35 (1974) C6-209.
[8] E. Gerdau, R. Rüffer, H. Winkler, W. Tolksdorf, C.P. Klages and J.P. Hannon, Phys. Rev. Lett. 54 (1985) 835.
[9] E. Gerdau and H. de Waard, eds., *Nuclear Resonant Scattering of Synchrotron Radiation*, Hyp. Interact. 123–125 (1999/2000).
[10] G.P. Srivastava, *The Physics of Phonons* (Adam Hilger, Bristol, UK, 1990).
[11] M. Seto, Y. Yoda, S. Kikuta, X.W. Zhang and M. Ando, Phys. Rev. Lett. 74 (1995) 3828.

[12] W. Sturhahn, T.S. Toellner, E.E. Alp, X.W. Zhang, M. Ando, Y. Yoda, S. Kikuta, M. Seto, C.W. Kimball and B. Dabrowski, Phys. Rev. Lett. 74 (1995) 3832.
[13] A.I. Chumakov, R. Rüffer, H. Grünsteudel, H.F. Grünsteudel, G. Grübel, J. Metge and H.A. Goodwin, Europhys. Lett. 30 (1995) 427.
[14] A.I. Chumakov and W. Sturhahn, this issue, section V-1.1.
[15] W. Keune and W. Sturhahn, this issue, section V-1.5.
[16] W. Sturhahn and A.I. Chumakov, this issue, section V-1.2.
[17] R.L. Cohen, G.L. Miller and K.W. West, Phys. Rev. Lett. 15 (1978) 381.
[18] U. Bergmann, J.B. Hastings and D.P. Siddons, Phys. Rev. B 49 (1994) 1513.
[19] A.Q.R. Baron, A.I. Chumakov, R. Rüffer, H. Grünsteudel, H.F. Grünsteudel and O. Leupold, Europhys. Lett. 34 (1996) 331.
[20] W. Sturhahn, K.W. Quast, T.S. Toellner, E.E. Alp, J. Metge and E. Gerdau, Phys. Rev. B 53 (1996) 171.
[21] U. Balucani and M. Zoppi, *Dynamics of the Liquid State* (Oxford Univ. Press, New York, 1994).
[22] L. Van Hove, Phys. Rev. 95 (1954) 249.
[23] J.P. Hannon and G.T. Trammell, Phys. Rev. 169 (1968) 315, and 186 (1969) 306.
[24] R.P. Feynman, *Quantum Electrodynamics* (Benjamin, New York, 1962).
[25] M. Gell-Mann and M.L. Goldberger, Phys. Rev. 96 (1953) 398.
[26] H.C. Goldwire, Jr. and J.P. Hannon, Phys. Rev. B 16 (1977) 1875.
[27] A.I. Chumakov, A. Barla, R. Rüffer, J. Metge, H.F. Grünsteudel, H. Grünsteudel, J. Plessel, H. Winkelmann and M.M. Abd-Elmeguid, Phys. Rev. B 58 (1998) 254.
[28] M.Y. Hu, T.S. Toellner, W. Sturhahn, P.M. Hession, J.P. Sutter and E.E. Alp, Nucl. Instrum. Methods A 430 (1999) 271.
[29] A.I. Chumakov, J. Metge, A.Q.R. Baron, R. Rüffer, Y.V. Shvyd'ko, H. Grünsteudel and H.F. Grünsteudel, Phys. Rev. B 56 (1997) R8455.
[30] J. Metge, Ph.D. thesis, Universität Hamburg (1996).
[31] J. Metge, private communication (1997).
[32] W. Sturhahn, unpublished (1998).
[33] Y. Kagan, private communication (1995).
[34] W. Sturhahn and T.S. Toellner, unpublished (1998).
[35] H.J. Lipkin, Ann. Phys. 9 (1960) 332, Phys. Rev. B 52 (1995) 10073.
[36] H.J. Lipkin, this issue, section III-2.1.
[37] N.W. Ashcroft and N.D. Mermin, *Solid State Physics* (W.B. Saunders Company, Philadelphia, PA, 1976).
[38] V.G. Kohn, A.I. Chumakov and R. Rüffer, Phys. Rev. B 58 (1998) 8437.
[39] T. Nakayama, K. Yakubo and R.L. Orbach, Rev. Mod. Phys. 66 (1994) 381.
[40] W. Schirmacher, G. Diezemann and C. Ganter, Phys. Rev. Lett. 81 (1998) 136.
[41] M. Weissbluth, *Photon–Atom Interactions* (Academic Press, San Diego, CA, 1989).
[42] M.E. Rose, *Elementary Theory of Angular Momentum* (Wiley, New York, 1957).
[43] H. Burzlaff, H. Zimmermann and P.M. de Wolff, in: *International Tables for Crystallography*, Vol. A, ed. T. Hahn (Kluwer Academic, Dordrecht, The Netherlands, 1996).